

Forbidden neutrino genesis

Shinya Kanemura^a and Shao-Ping Li^a

^aDepartment of Physics, Osaka University, Toyonaka, Osaka 560-0043, Japan

*E-mail: kanemu@het.phys.sci.osaka-u.ac.jp,
lisp@het.phys.sci.osaka-u.ac.jp*

ABSTRACT: The origin of neutrino masses can be simply attributed to a new scalar beyond the Standard Model. We demonstrate that leptogenesis can explain the baryon asymmetry of the universe already in such a minimal framework, where the electroweak scalar is favored to enhance the baryon asymmetry. Different from traditional leptogenesis, the realization here exploits the thermal behavior of leptons at finite temperatures, which is otherwise kinetically forbidden in vacuum. We present detailed calculations of the CP asymmetry in the Schwinger-Keldysh Closed-Time-Path formalism, and compute the asymmetry evolution via the Kadanoff-Baym equation. Such minimal forbidden neutrino genesis establishes a direct link between the baryon asymmetry and the CP-violating phase from neutrino mixing, making the scenario a compelling target in neutrino oscillation experiments. Complementary probes from cosmology, flavor physics and colliders are also briefly discussed.

Contents

| | | |
|----------|---|-----------|
| 1 | Introduction | 1 |
| 2 | A minimal neutrinophilic scalar scenario | 2 |
| 3 | Resonant forbidden leptogenesis | 5 |
| 3.1 | Kadanoff-Baym equation | 5 |
| 3.2 | One-loop washout rate | 6 |
| 3.3 | Two-loop CP-violating source from the PMNS phase | 8 |
| 3.4 | Nonthermal conditions | 10 |
| 3.5 | Neutrino asymmetries | 12 |
| 3.5.1 | Three nonthermal neutrinos | 12 |
| 3.5.2 | One nonthermal neutrino | 16 |
| 4 | Discussions | 18 |
| 4.1 | Comparison with the Boltzmann equation | 18 |
| 4.2 | Phenomenology | 19 |
| 5 | Conclusion | 23 |
| A | Propagators in the SK-CTP formalism | 24 |
| B | Soft-lepton resummation in Hard-Thermal-Loop approximation | 25 |
| C | CP-violating rate from three nonthermal neutrinos | 29 |

1 Introduction

Baryogenesis via leptogenesis [1–3] is a simple mechanism that can explain the baryon asymmetry of the universe (BAU), which typically occurs above the sphaleron decoupling temperature $T_{\text{sph}} \approx 132$ GeV [4, 5]. While the study of leptogenesis is mostly based on perturbative lepton-number violation [6–9], leptogenesis can also be realized with a total lepton number conserved and shared between the Standard Model (SM) and a hidden sector. Such lepton-number conserving leptogenesis can also feature connections to the neutrino mass origin when the hidden sector consists of light Majorana or Dirac right-handed neutrinos [10, 11], and links to dark matter co-generation [12, 13].

Leptogenesis is a high-temperature process, where finite-temperature corrections should generally contribute to the generation of CP asymmetries. Theoretical development of leptogenesis in recent years confirms this expectation, and has brought us an interesting phenomenon: the CP asymmetry at high temperatures can be induced by a pure plasma effect that would be otherwise kinetically forbidden in vacuum. Generally, such a kind of *forbidden leptogenesis* can be exploited by using nonthermal quantum field theory, or the Schwinger-Keldysh Closed-Time-Path (SK-CTP) formalism [14–16], as mostly studied in lepton-number violating scenarios [17–28].

Based on the SK-CTP formalism, the evolution of CP asymmetries is determined by the Kadanoff-Baym (KB) equation, which is more technically and computationally challenging than the conventional Boltzmann equation. However, the KB equation does not suffer from the double-counting issue found in the Boltzmann equation, which is related to the real-intermediate-state subtraction [6, 29]. Instead, the KB collision rates automatically include all the relevant processes from two-loop diagrams, where the subtraction of on-shell scattering is guaranteed [13, 18].

Regarding the complexity of finite-temperature CP asymmetries, it is recently pointed out in Ref. [13] that if the total lepton number is (nearly) conserved and shared between the SM leptons and hidden particles, the origin of CP asymmetries in forbidden leptogenesis will become easy to trace. In that regime, one can use perturbative lepton-number conservation to calculate the hidden asymmetries, where a resonant enhancement from soft-lepton resummation clearly shows up in two-loop self-energy diagrams. In contrast to resonant leptogenesis via vacuum mass degeneracy [30, 31], the appearance of soft-lepton resonance is itself a SM prediction and the resonant enhancement is protected from finite width under perturbative finite-temperature field theory.

A compelling feature of forbidden leptogenesis is that CP asymmetries can be generated with minimal particle physics, where traditional leptogenesis based on vacuum quantum field theory cannot be realized. Consequently, forbidden leptogenesis can open more channels to explain the BAU without invoking abundant particle content. This comes from the expectation that finite-temperature corrections induce more absorptive contributions (kinetic phases) than from vacuum loop diagrams. It also implies that in non-minimal particle-physics scenarios considered insofar, forbidden leptogenesis can readily contribute an irreducible CP asymmetry at high temperatures, which in some cases could even dominate over the conventional CP asymmetry and hence should be considered consistently whenever traditional leptogenesis is at work.

In this paper, we consider forbidden leptogenesis in a minimal framework, where a new neutrinophilic scalar is introduced to the SM. Concretely, we consider a two-Higgs-doublet model with right-handed neutrinos, in which the vacuum expectation value of the second Higgs doublet gives Dirac masses to SM neutrinos [32, 33]. Both right-handed neutrinos and their asymmetries are co-generated via neutrinophilic scalar decay, and hence is dubbed *forbidden leptogenesis*. The total lepton number is conserved and shared between the SM lepton and right-handed neutrino sectors. In such a minimal neutrinophilic scalar scenario, the CP violation for the BAU is sourced by the Pontecorvo–Maki–Nakagawa–Sakata (PMNS) mixing matrix [34, 35]. In particular, the Dirac CP-violating phase in the PMNS matrix determines the sign of the baryon asymmetry, making this scenario highly falsifiable in terms of neutrino oscillation experiments.

We begin in section 2 with the introduction of the neutrinophilic scalar scenario. Section 3 is devoted to elaborating the calculations of forbidden leptogenesis in the SK-CTP formalism with the KB equation, where the resonant enhancement from soft-lepton resummation can be traced. In section 4.1, we will make a comparison between the KB and Boltzmann equations, pointing out some issues in previous work. In section 4.2, we will briefly discuss some phenomenological signals, showing the complementary probes in cosmology, flavor physics and colliders. Finally, we will present the conclusions in section 5. The propagators and resummation in the SK-CTP formalism, as well as some technical calculations of finite-temperature CP asymmetries used in section 3 will be relegated to some appendices.

2 A minimal neutrinophilic scalar scenario

One of the simplest explanations for the SM neutrino masses is to introduce a second Higgs doublet beyond the SM [32, 33]. Right-handed neutrinos would exclusively couple to the second Higgs

doublet ϕ_2 if some hidden symmetry exists. For example, a global $U(1)$ or Z_2 symmetry in the (ν_R, ϕ_2) sector will forbid ν_R from coupling to the SM-like Higgs doublet ϕ_1 , and will also prevent ϕ_2 from coupling to the SM quarks and right-handed charged-lepton singlets. Furthermore, the hidden symmetry dictates a simple structure of the scalar potential:

$$V(\phi_1, \phi_2) = \mu_1^2 \phi_1^\dagger \phi_1 + \mu_2^2 \phi_2^\dagger \phi_2 + \frac{\lambda_1}{2} (\phi_1^\dagger \phi_1)^2 + \frac{\lambda_2}{2} (\phi_2^\dagger \phi_2)^2 + \lambda_3 (\phi_1^\dagger \phi_1) (\phi_2^\dagger \phi_2) + \lambda_4 (\phi_1^\dagger \phi_2) (\phi_2^\dagger \phi_1) + \left[-\mu^2 \phi_1^\dagger \phi_2 + \frac{\lambda_5}{2} (\phi_1^\dagger \phi_2)^2 + \text{h.c.} \right], \quad (2.1)$$

where by definition $\mu_1^2 < 0$, $\mu_2^2 > 0$ and $\mu^2 > 0$ [33, 36, 37]. The terms in the square brackets denote the low-scale effective interactions, where the hidden symmetry is explicitly broken. These terms may be induced via a super-renormalizable portal to inflaton field ϕ_{inf} through $\mu_{\text{UV}} (\phi_1^\dagger \phi_2) \phi_{\text{inf}}$, with μ_{UV} a dimensionful coupling at high scales. This super-renormalizable portal could open interesting connections to high-scale physics, such as spontaneous symmetry breaking and the associated topological defects. In this paper, we will turn agnostic on the origin of the symmetry-breaking terms in the square brackets, and simply take μ^2, λ_5 as free parameters.

The neutrino Yukawa interaction is built upon the following lepton portal [32, 33]:

$$\mathcal{L} = -y_{i\alpha} \bar{\ell}_i \tilde{\phi}_2 \nu_{R\alpha} + \text{h.c.}, \quad (2.2)$$

where $\nu_{R\alpha}$ are the three right-handed Dirac counterparts of the SM left-handed neutrinos, and $\tilde{\phi}_2 \equiv i\sigma_2 \phi_2^*$ with σ_2 the second Pauli matrix. For Dirac neutrinos with perturbative lepton-number conservation, there is no Majorana mass term $m \bar{\nu}_R^c \nu_R$ accompanied.

Although the hidden symmetry may not be mandatory by nature, it makes the Yukawa interaction (2.2) a minimal and distinguishable scenario from the traditional two-Higgs-doublet models (see Ref. [37] for a review). It is worth mentioning that without the hidden symmetry right-handed neutrinos also couple to ϕ_1 which, as will be shown later, corresponds the SM Higgs doublet having the vacuum expectation value $v_1 \approx 246$ GeV, but such interactions are experimentally less interesting and irrelevant due to the exceedingly weak Yukawa couplings $\lesssim \mathcal{O}(10^{-13})$, even though the feebleness of neutrino Yukawa couplings is technically natural on the theoretical side. This is one of the motivations for introducing the second Higgs doublet with some hidden symmetry, where the vacuum expectation value can be much smaller than v_1 and hence the neutrino Yukawa couplings can be larger by orders of magnitude.

The Higgs doublets from Eq. (2.1) can be parameterized as

$$\phi_a = \begin{pmatrix} \varphi_a^+ \\ \frac{1}{\sqrt{2}}(v_a + \rho_a + i\eta_a) \end{pmatrix}, \quad a = 1, 2, \quad (2.3)$$

where the vacuum expectation values satisfy $(v_1^2 + v_2^2)^{1/2} = 246$ GeV. In the limit of $v_1 \gg v_2, \mu$, the tadpole equations yield

$$v_1 \approx \sqrt{-\frac{2\mu_1^2}{\lambda_1}}, \quad v_2 \approx \frac{2\mu^2 v_1}{2\mu_2^2 + \lambda_+ v_1^2}, \quad (2.4)$$

with $\lambda_+ \equiv \lambda_3 + \lambda_4 + \lambda_5$. The mixed charged components will give rise to charged Goldstone bosons (G^\pm) and physical charged scalars (H^\pm), while the mixed η_a fields lead to one neutral

Goldstone boson (G^0) and one pseudoscalar (A). The transformation rules read

$$\begin{pmatrix} \varphi_1^\pm \\ \varphi_2^\pm \end{pmatrix} = \begin{pmatrix} \cos \beta & -\sin \beta \\ \sin \beta & \cos \beta \end{pmatrix} \begin{pmatrix} G^\pm \\ H^\pm \end{pmatrix}, \quad \begin{pmatrix} \eta_1 \\ \eta_2 \end{pmatrix} = \begin{pmatrix} \cos \beta & -\sin \beta \\ \sin \beta & \cos \beta \end{pmatrix} \begin{pmatrix} G^0 \\ A \end{pmatrix}, \quad (2.5)$$

where the mixing angle is given by

$$\tan \beta = \frac{v_2}{v_1}. \quad (2.6)$$

On the other hand, the mixed ρ_a fields give rise to the SM Higgs boson (h) and a new scalar boson (H), with the transformation defined by

$$\begin{pmatrix} \rho_1 \\ \rho_2 \end{pmatrix} = \begin{pmatrix} \cos \alpha & -\sin \alpha \\ \sin \alpha & \cos \alpha \end{pmatrix} \begin{pmatrix} h \\ H \end{pmatrix}. \quad (2.7)$$

The mixing angle α is found to be

$$\tan(2\alpha) = \frac{4(\mu^2 - \lambda_+ v_1 v_2)}{(-3\lambda_1 + \lambda_+)v_1^2 - 2\mu_1^2 + 2\mu_2^2 + 3\lambda_2 v_2^2 - \lambda_+ v_2^2} \quad (2.8)$$

$$\approx \frac{2v_2(2\mu_2^2/v_1 - \lambda_+ v_1)}{(-2\lambda_1 + \lambda_+)v_1^2 + 2\mu_2^2}, \quad (2.9)$$

where the second approximation is derived in the limit of $v_1 \gg v_2, \mu$. For $\mu_2 \gtrsim v_1$, we arrive at

$$\tan(2\alpha) \simeq \mathcal{O}(v_2/v_1), \quad (2.10)$$

indicating that mixing of h and H is suppressed and ϕ_1 will reduce to the SM Higgs doublet (denoted by ϕ_{SM}) while ϕ_2 becomes a neutrinophilic Higgs doublet (denoted by ϕ),

$$\phi_1 \approx \phi_{\text{SM}}, \quad \phi_2 \approx \phi. \quad (2.11)$$

After gauge symmetry breaking, SM neutrinos acquire masses from ϕ , with

$$m = \frac{y}{\sqrt{2}} v_2. \quad (2.12)$$

In the following analysis, we will take the alignment limit given by Eq. (2.11), which will be justified by $v_2 \ll v_1$ inferred from forbidden neutrino genesis. In the limit of Eq. (2.11), the mass spectrum of the Higgs bosons reads

$$m_h^2 \approx \lambda_1 v_1^2, \quad m_H^2 \approx \mu_2^2 + \frac{\lambda_+}{2} v_1^2, \quad m_A^2 \approx \mu_2^2 + \frac{\lambda_-}{2} v_1^2, \quad m_{H^\pm}^2 \approx \mu_2^2 + \frac{\lambda_3}{2} v_1^2, \quad (2.13)$$

where $\lambda_- \equiv \lambda_3 + \lambda_4 - \lambda_5$.

The λ parameters in Eq. (2.1) are theoretically constrained by the requirements of vacuum stability [37–40], triviality [41–45], and also by perturbative unitarity [46–49]. In addition, there are experimental constraints on the Higgs mass spectrum. In particular, the electroweak corrections, which are commonly parameterized by the oblique parameters [50–53], require a quasi-degenerate mass between H^\pm and A/H [54–56]. Direct searches from the LEP collaborations have also excluded a charged-scalar mass below 80 GeV [57]. These constraints will be considered in the

following analysis, which helps to determine whether the forbidden neutrinogenesis can be realized in the minimal neutrinophilic scalar scenario.

3 Resonant forbidden neutrinogenesis

Due to lepton-number conservation, the SM lepton asymmetries generated via the Yukawa interaction (2.2) will be accompanied by right-handed neutrino asymmetries. As long as the asymmetry in the right-handed neutrino sector is maintained by the out-of-equilibrium condition persisted prior to sphaleron decoupling, there would also be a net asymmetry in the SM lepton sector. The SM lepton asymmetry will be converted into the baryon asymmetry via active sphaleron processes, while the asymmetry in the right-handed neutrino sector accumulates over time. Even though the SM leptons are in quasi-thermal equilibrium, the net SM lepton asymmetry would not be washed out before sphaleron processing. Instead, it will be redistributed among lepton flavors.

The final baryon asymmetry is simply determined by the amount of asymmetries stored in the ν_R sector. Based on the sphaleron conversion efficiency, chemical equilibrium and perturbative lepton-number conservation, one can obtain the relation between the baryon and right-handed neutrino asymmetries [58]:

$$Y_B \equiv \frac{n_B - n_{\bar{B}}}{s_{\text{SM}}} \approx 0.35 \sum_{\alpha} Y_{\nu_{R\alpha}}, \quad (3.1)$$

where $Y_{\nu_{R\alpha}} \equiv (n_{\nu_{R\alpha}} - n_{\bar{\nu}_{R\alpha}})/s_{\text{SM}}$ denotes the ν_R asymmetry of flavor α normalized to the SM entropy density,

$$s_{\text{SM}} = g_s(T) \frac{2\pi^2}{45} T^3, \quad (3.2)$$

with $g_s(T)$ the effective degrees of freedom. Typically, we have $g_s(T) \approx 106.75$ during leptogenesis. The total ν_R asymmetry should match the observed Y_B at present day [59]:

$$Y_B \approx 8.75 \times 10^{-11}. \quad (3.3)$$

In addition, one can circumvent the dynamics of asymmetry redistribution in SM lepton flavors, using the evolution of the accompanying ν_R asymmetry as a result of perturbative lepton-number conservation. This technical treatment will allow us to visualize the role of resummed thermal leptons in contributing to finite-temperature CP asymmetries.

3.1 Kadanoff-Baym equation

To calculate the CP asymmetry in the ν_R sector, we start from the KB kinetic equation for right-handed Dirac neutrinos [13, 18, 60, 61]:

$$\gamma^0 \frac{d}{dt} (i\cancel{\mathcal{G}}_{\nu\alpha}^{\leq}) = (-i\cancel{\Sigma}_{\nu\alpha}^>)(i\cancel{\mathcal{G}}_{\nu\alpha}^<) - (-i\cancel{\Sigma}_{\nu\alpha}^<)(i\cancel{\mathcal{G}}_{\nu\alpha}^>), \quad (3.4)$$

where $i\cancel{\mathcal{G}}_{\nu\alpha}^{\leq}$ denote the Wightman functions and $-i\cancel{\Sigma}_{\nu\alpha}^{\gtrless}$ the self-energy amplitudes for ν_R of flavor α , with the slashed symbol highlighting the spinor structures of fermion self-energy amplitudes and propagators. Notice that $d(i\cancel{\mathcal{G}}_{\nu\alpha}^<)/dt$ and $d(i\cancel{\mathcal{G}}_{\nu\alpha}^>)/dt$ have the same rate from the right-hand side.

The particle-number asymmetry of right-handed neutrinos, $\Delta n_\alpha \equiv n_{\nu_\alpha} - n_{\bar{\nu}_\alpha}$, can be obtained from Eq. (3.4) by integrating over the 4-momentum of neutrinos and performing the Dirac trace, which gives rise to

$$\frac{d\Delta n_\alpha}{dt} = \frac{1}{2} \int_p \text{Tr} \left[i\mathcal{Y}_{\nu_\alpha}^> i\mathcal{S}_{\nu_\alpha}^< - i\mathcal{Y}_{\nu_\alpha}^< i\mathcal{S}_{\nu_\alpha}^> \right], \quad (3.5)$$

with Tr being the Dirac trace and

$$\int_p \equiv \int \frac{d^4 p}{(2\pi)^4}, \quad (3.6)$$

for shorthand. The KB collision rates on the right-hand side of Eq. (3.5) contain the washout effect at one-loop level and the CP-violating source at two-loop level.

3.2 One-loop washout rate

The washout processes are determined by the one-loop self-energy diagrams of ν_α , as shown in Fig. 1. The one-loop amplitudes $\mathcal{Y}_{\nu_\alpha}^{\lessgtr}$ read¹

$$i\mathcal{Y}_{\nu_\alpha}^{+-}(p) \equiv i\mathcal{Y}_{\nu_\alpha}^<(p) = 2|y_\alpha|^2 \int_{p_\ell} \int_{p_\phi} (2\pi)^4 \delta^4(p - p_\ell + p_\phi) P_L i\mathcal{S}_\ell^< P_R iG_\phi^>, \quad (3.7)$$

$$i\mathcal{Y}_{\nu_\alpha}^{-+}(p) \equiv i\mathcal{Y}_{\nu_\alpha}^>(p) = 2|y_\alpha|^2 \int_{p_\ell} \int_{p_\phi} (2\pi)^4 \delta^4(p - p_\ell + p_\phi) P_L i\mathcal{S}_\ell^> P_R iG_\phi^<, \quad (3.8)$$

where $(+-), (-+)$ denote the thermal indices, and the factor of 2 comes from gauge $SU(2)_L$ degeneracy. The Yukawa coupling is defined as

$$|y_\alpha|^2 \equiv \sum_{i=e,\mu,\tau} y_{i\alpha} y_{i\alpha}^*, \quad (3.9)$$

and $\mathcal{S}_\ell^{\lessgtr}, G_\phi^{\lessgtr}$ denote the lepton and scalar propagators collected in Appendix A.

Calculating the one-loop self-energy amplitudes straightforwardly, we obtain the washout rate:

$$\begin{aligned} \mathcal{W} &= \frac{1}{2} \int_p \text{Tr} \left[i\mathcal{Y}_{\nu_\alpha}^> i\mathcal{S}_{\nu_\alpha}^< - i\mathcal{Y}_{\nu_\alpha}^< i\mathcal{S}_{\nu_\alpha}^> \right]_{1\text{-loop}} \\ &= -\frac{|y_\alpha|^2 m_\phi^2}{32\pi^3} \int_0^\infty dp \int_{m_\phi^2/(4p)}^\infty dp_\ell [f_\alpha(p) - \bar{f}_\alpha(p)] \left[f_\phi^{\text{eq}}(p_\ell + p) + f_\ell^{\text{eq}}(p_\ell) \right], \end{aligned} \quad (3.10)$$

where we have used $\text{Tr}[P_L \not{p}_\ell P_R \not{p}] = -m_\phi^2$ and the Dirac δ -functions dictate the energy threshold: $p_0 p_{\ell 0} < 0$. The integration limit of $p_\ell \equiv |\vec{p}_\ell|$ comes from the angular integral via the Dirac δ -function in G_ϕ^{\lessgtr} . The washout effect from Eq. (3.10) exhibits the expected scaling $f_\alpha - \bar{f}_\alpha$, which, in the absence of the CP-violating source, implies that Δn_α will be diluted exponentially.

In the weak washout regime where $\nu_{R\alpha}$ is not initially present in the thermal plasma, both f_α and \bar{f}_α are negligible due to the small Yukawa couplings. In the early stage, there is no significant

¹An easy way to remember the correspondence between the thermal indices \pm and the symbols \lessgtr is that the time variable for $+$ in the SK-CTP formalism is always earlier (smaller $<$) than for $-$.

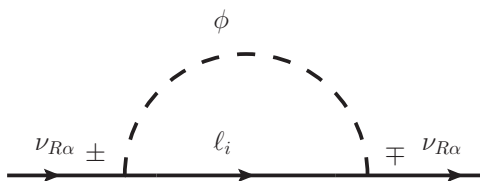


Figure 1. The one-loop self-energy diagram of $\nu_{R\alpha}$ contributing to the washout rate. The thermal indices $+-$ and $-+$ correspond to the amplitudes $\mathcal{Y}_{\nu_\alpha}^<$ and $\mathcal{Y}_{\nu_\alpha}^>$, respectively.

generation of CP asymmetries. When $T \lesssim m_\phi$, f_α , \bar{f}_α and their difference increase. In the limit of $m_\phi \gg T$, the p_ℓ -integration would yield

$$\int_{m_\phi^2/(4p)}^{\infty} \left[f_\phi^{\text{eq}}(p_\ell + p) + f_\ell^{\text{eq}}(p_\ell) \right] = T \ln \left(\frac{e^{m_\phi^2/(4pT)} + 1}{e^{m_\phi^2/(4pT) + p/T} - 1} \right) + p \approx 0, \quad (3.11)$$

where $p = m_\phi/2$ was used in the last approximation. Therefore, we see that in the weak washout regime \mathcal{W} is suppressed by $f_\alpha - \bar{f}_\alpha$ at early times and then it becomes suppressed by the p_ℓ -integration at later times even if f_α and \bar{f}_α can approach the equilibrium state.

However, if right-handed neutrinos reach thermal equilibrium already at $T > m_\phi$, the washout effect would become strong and the depletion of the generated ν_R asymmetries towards the end of neutrino genesis should be taken into account. Once right-handed neutrinos become fully thermalized, the CP-violating source would vanish, leaving the washout rate \mathcal{W} to exponentially dilute the ν_R asymmetry. To see this, we notice

$$f_\alpha(p) - \bar{f}_\alpha(p) \approx 12 \frac{n_\alpha - \bar{n}_\alpha}{T^3} \frac{e^{p/T}}{(e^{p/T} + 1)^2}, \quad (3.12)$$

at leading order of a small chemical potential. Replacing d/dt with $\partial/\partial t + 3\mathcal{H}$ in Eq. (3.5), where \mathcal{H} is the Hubble parameter

$$\mathcal{H} \approx 1.66 \sqrt{g_\rho(T)} \frac{T^2}{m_{\text{P}}}, \quad (3.13)$$

with $m_{\text{P}} \approx 1.22 \times 10^{19}$ GeV the Planck mass and $g_\rho(T)$ the effective degrees of freedom in energy,² we can evaluate the washout with $\mathcal{S}_{\text{CP}} = 0$, giving rise to

$$Y_{\nu_\alpha}(z_f) = Y_{\nu_\alpha}(z_i) e^{-\tilde{\mathcal{W}}}, \quad \tilde{\mathcal{W}} = \left(\frac{|y_\alpha|}{10^{-6}} \right)^2 \left(\frac{8.45 \text{ TeV}}{m_\phi} \right) I(z_i, z_f), \quad (3.14)$$

$$I(z_i, z_f) = \int_{z_i}^{z_f} z^2 dz \int_0^\infty dx_\alpha \int_{z^2/(4x_\alpha)}^\infty dx_\ell \frac{e^{x_\alpha}}{(e^{x_\alpha} + 1)^2} \left[f_\phi^{\text{eq}}(x_\ell + x_\alpha) + f_\ell^{\text{eq}}(x_\ell) \right]. \quad (3.15)$$

$Y_{\nu_\alpha}(z_i)$ is the $\nu_{R\alpha}$ asymmetry initially generated at $z_i \equiv m_\phi/T_i$, and $Y_{\nu_\alpha}(z_f)$ is the final asymmetry at $z_f \equiv m_\phi/T_{\text{sph}}$. Here we introduce the dimensionless variables $x_\alpha \equiv p/T$ and $x_\ell \equiv p_\ell/T$.

We show in Fig. 2 the washout effect in terms of z_i and m_ϕ by fixing $|y_\alpha| = 10^{-6}$. We see that when neutrino genesis completes at $z_i < 1$ due to ν_R thermalization, a lighter scalar generally

²We will take $g_\rho \approx g_s$ in the computation of Y_ν .

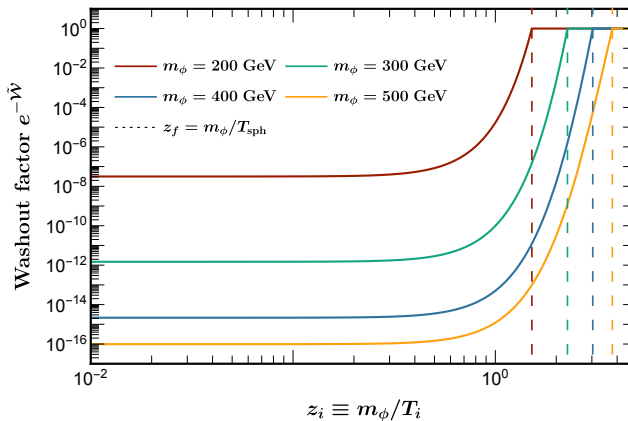


Figure 2. The washout factor $e^{-\tilde{W}}$ towards sphaleron decoupling, where forbidden neutrino genesis completes at $z_i = m_\phi/T_i$. The vertical lines correspond to sphaleron decoupling at $z_f = m_\phi/T_{\text{sph}}$.

results in a smaller dilution factor $e^{-\tilde{W}}$ and hence a smaller washout effect. However, a scalar as light as 200 GeV would still predict a dilution of ν_R asymmetry by a factor of 10^3 if ν_R has already reached thermal equilibrium at $z_i < 1.22$. To ensure the washout effect with a dilution factor less than, *e.g.*, 10, $z_i \gtrsim 1.42$ is required for $m_\phi = 200$ GeV, which is close to sphaleron decoupling at $z_f = 1.52$. When the scalar mass increases to 500 GeV, a huge dilution factor 10^{16} would arise if neutrino genesis completes at $z_i < 1$, rendering a vanishing ν_R asymmetry. A dilution factor less than 10 for $m_\phi = 500$ GeV requires neutrino genesis completes after $z_i \approx 3.61$, which however cannot be realized due to earlier ν_R thermalization, as will be discussed in section 3.4. While this could be resolved by taking a smaller Yukawa coupling, the CP-violating source will also be suppressed at the same time.

The results shown in Fig. 2 will provide an easy way to check whether the strong washout effect arises for a given scalar mass. This circumvents the numerical computation of the full integro-differential KB equation.

3.3 Two-loop CP-violating source from the PMNS phase

In this section, we will first present the general formula for the CP-violating source. Then we discuss the dependence of CP asymmetries on the Yukawa phase, which is unique in the minimal neutrophilic scalar scenario. After that, we will elaborate the general result in section 3.5, after the nonthermal conditions are specified in section 3.4.

In the SK-CTP formalism, the leading-order CP-violating source starts at two-loop level. The two-loop self-energy diagrams that can induce ν_R asymmetries are determined by Fig. 3. The amplitudes read

$$i\mathcal{Z}_{\nu_\alpha}^<(p) = 2y_4 \int_{p_\ell} \int_{p_\phi} (2\pi)^4 \delta^4(p - p_\ell + p_\phi) P_L i\mathcal{S}_{\ell_{ij}}^< P_R iG_\phi^>, \quad (3.16)$$

$$i\mathcal{Z}_{\nu_\alpha}^>(p) = 2y_4^* \int_{p_\ell} \int_{p_\phi} (2\pi)^4 \delta^4(p - p_\ell + p_\phi) P_L i\mathcal{S}_{\ell_{ji}}^> P_R iG_\phi^<, \quad (3.17)$$

where the factor of 2 comes from gauge $SU(2)_L$ degeneracy. The Yukawa coupling y_4 is defined

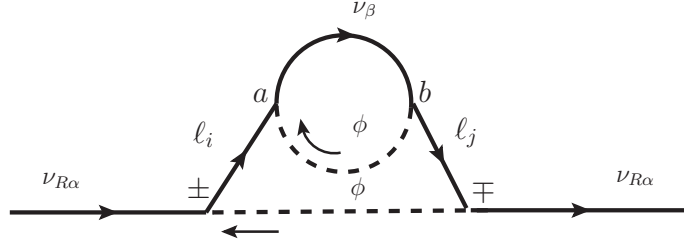


Figure 3. The two-loop self-energy diagram of $\nu_{R\alpha}$ contributing to the forbidden CP asymmetry. The outer thermal indices \pm correspond to the amplitudes $\mathcal{Y}_{\nu_\alpha}^{\leq}$. The inner vertices a, b are summed over thermal indices \pm , generating terms given in Eqs. (3.19)-(3.20). We use the arrows for the scalar propagators to denote the momentum flow, and make the fermion arrows align with the momentum flow.

by

$$y_4 \equiv y_{i\alpha} y_{j\alpha}^* y_{i\beta}^* y_{j\beta}, \quad (3.18)$$

and we have played the trick of interchanging dummy indices i, j in $i\mathcal{Y}_{\nu_\alpha}^>$ such that the dependence on the Yukawa couplings is complex-conjugated to that in $i\mathcal{Y}_{\nu_\alpha}^<$. Such a difference will lead to the common expectation that the CP-violating source depends on the Yukawa phase, i.e., $\text{Im}(y_4)$.

In Eqs. (3.16)-(3.17), $i\mathcal{S}_{\ell_{ij}}^<$ and $i\mathcal{S}_{\ell_{ji}}^>$ comprise the product of resummed lepton propagators and the inner loop amplitudes. Summing the thermal indices $a, b = \pm$ in the inner loop gives arise to³

$$\begin{aligned} i\mathcal{S}_{\ell_{ij}}^< &= (i\mathcal{S}_{\ell_i}^R)(-i\mathcal{Y}_\ell^T)(i\mathcal{S}_{\ell_j}^<) + (i\mathcal{S}_{\ell_i}^R)(-i\mathcal{Y}_\ell^<)(i\mathcal{S}_{\ell_j}^R) + (i\mathcal{S}_{\ell_i}^<)(-i\mathcal{Y}_\ell^<)(i\mathcal{S}_{\ell_j}^R) \\ &\quad - (i\mathcal{S}_{\ell_i}^R)(-i\mathcal{Y}_\ell^<)(i\mathcal{S}_{\ell_j}^>) - (i\mathcal{S}_{\ell_i}^<)(-i\mathcal{Y}_\ell^T)(i\mathcal{S}_{\ell_j}^R), \end{aligned} \quad (3.19)$$

$$\begin{aligned} i\mathcal{S}_{\ell_{ji}}^> &= (i\mathcal{S}_{\ell_i}^R)(-i\mathcal{Y}_\ell^T)(i\mathcal{S}_{\ell_j}^>) + (i\mathcal{S}_{\ell_i}^R)(-i\mathcal{Y}_\ell^>)(i\mathcal{S}_{\ell_j}^R) + (i\mathcal{S}_{\ell_i}^<)(-i\mathcal{Y}_\ell^>)(i\mathcal{S}_{\ell_j}^R) \\ &\quad - (i\mathcal{S}_{\ell_i}^R)(-i\mathcal{Y}_\ell^>)(i\mathcal{S}_{\ell_j}^>) - (i\mathcal{S}_{\ell_i}^>)(-i\mathcal{Y}_\ell^T)(i\mathcal{S}_{\ell_j}^R), \end{aligned} \quad (3.20)$$

where $\mathcal{S}_{\ell_i}^{R,\leq}$ denote the resummed retarded and Wightman propagators of lepton i , and the Yukawa couplings from the inner loop amplitudes $-i\mathcal{Y}_{\ell_{ij}}^{ab}$ have been factored out and absorbed into y_4 , with

$$\mathcal{Y}_{\ell_{ij}}^{ab} \equiv y_{i\beta}^* y_{j\beta} \mathcal{Y}_\ell^{ab}, \quad a, b = \pm. \quad (3.21)$$

To calculate the CP asymmetry with resummed thermal leptons, it is beneficial to take a proper basis where thermal corrections to leptons are diagonal in flavor space. To this aim, we choose the basis where the charged-lepton Yukawa matrix is diagonal. When the thermal mass correction to leptons is dominated by the SM contributions (gauge and charged-lepton Yukawa interactions), the basis we choose will make both the lepton thermal mass matrix and the resummed lepton propagators diagonal in flavor space [62]. In this basis, the neutrino Yukawa matrix y given in

³See also the Supplemental Material in Ref. [13].

Eq. (2.2) and the physical PMNS matrix would be related via⁴

$$y_{ij} = \frac{\sqrt{2}}{v_2} U_{ij} m_j, \quad (3.22)$$

where m_j represents the physical neutrino masses, and we have used unitary PMNS matrix $U^\dagger U = UU^\dagger = 1$. In the standard parameterization, U is given by [63]

$$U = \begin{pmatrix} c_{12}c_{13} & s_{12}c_{13} & e^{-i\delta_{\text{CP}}}s_{13} \\ -s_{12}c_{23} - e^{i\delta_{\text{CP}}}c_{12}s_{13}s_{23} & c_{12}c_{23} - e^{i\delta_{\text{CP}}}s_{12}s_{13}s_{23} & c_{13}s_{23} \\ s_{12}s_{23} - e^{i\delta_{\text{CP}}}c_{12}s_{13}c_{23} & -c_{12}s_{23} - e^{i\delta_{\text{CP}}}s_{12}s_{13}c_{23} & c_{13}c_{23} \end{pmatrix}, \quad (3.23)$$

where $s_{ij} \equiv \sin \theta_{ij}$ and $c_{ij} \equiv \cos \theta_{ij}$ correspond to the mixing angles, while δ_{CP} is the Dirac CP-violating phase that could feature large CP violation in the lepton sector. Then we can rewrite the Yukawa couplings as

$$|y_\alpha|^2 \equiv \sum_i y_{i\alpha} y_{i\alpha}^* = \frac{2}{v_2^2} |U_{i\alpha}|^2 m_\alpha^2, \quad (3.24)$$

$$\text{Im}(y_4) = \frac{4}{v_2^4} \text{Im} (U_{i\alpha} U_{j\alpha}^* U_{i\beta}^* U_{j\beta}) m_\alpha^2 m_\beta^2, \quad (3.25)$$

where $\text{Im}(y_4)$ represents the Yukawa phase for the CP asymmetry. Clearly, the Dirac CP-violating phase provides the unique source for CP violation in generating the ν_R asymmetry. If CP conservation from neutrino oscillation experiments is confirmed, forbidden leptogenesis will not work to explain the BAU in the minimal neutrinophilic scalar scenario.

Notice that in Eq. (3.25) the indices i, j, α, β should not be summed trivially, since the CP-violating source will carry additional dependence on these indices from lepton thermal masses and neutrino distribution functions, both of which are crucial to induce a nonzero CP-violating source. In fact, if the indices i, j can be summed trivially in Eq. (3.25), we would arrive at $\sum_{i,j} \text{Im}(y_4) = 0$. However, the flavor-dependent lepton thermal masses introduce additional i, j dependence, which, arising from Eqs. (3.19)-(3.20), is a key point in forbidden leptogenesis, and more generally in lepton-number conserving forbidden leptogenesis. We should emphasize that the lepton thermal masses are not inserted by hand,⁵ but is a consistent requirement from the two-particle-irreducible effective action constructed in the SK-CTP formalism [13, 16].

3.4 Nonthermal conditions

In addition to the PMNS phase as the source for CP violation, the nonthermal condition is also mandatory to realize leptogenesis in the early universe. Before elaborating the CP-violating source, we should determine the nonthermal conditions in the minimal neutrinophilic scalar scenario.

First of all, unlike the SM Higgs boson, the neutrinophilic scalar has a vacuum mass ($m_\phi = \mu_2$) before electroweak gauge symmetry breaking. Under cosmic expansion, the mass will drive the scalar into the out-of-equilibrium regime when the temperature drops to m_ϕ , providing a non-thermal condition for leptogenesis. However, to ensure an asymmetry in the ν_R sector, at least one of the right-handed neutrinos must be also out of equilibrium [13]. Then how many ν_R flavors are

⁴Recall that the PMNS matrix is defined in the weak charged current: $\bar{e}_i \gamma^\mu P_L U_{ij} \nu_j W_\mu^+ + \text{h.c.}$ for $e_i = e, \mu, \tau$.

⁵This treatment is often taken in the calculation of S -matrix amplitudes, where thermal masses are empirically inserted into the Feynman propagators [62].

sufficient to generate the requisite BAU? To answer this, we should recall the neutrino mass spectrum observed in neutrino oscillations [64]. Currently, the lightest neutrino mass, either in normal ordering or inverted ordering, is not determined yet by experiments, but it has an upper limit when imposing the bound from cosmology $\sum_i m_i < 0.12$ eV [59], which is $m_{1,\max} \approx 0.03$ eV in the normal ordering and $m_{3,\max} \approx 0.02$ eV in the inverted ordering. For the lightest neutrino mass ranging from the maximal value to zero, the other two heavier neutrinos do not exhibit strong mass hierarchy. Given Eq. (2.12), the Yukawa couplings of the two heavier neutrinos would be at the similar order, indicating that they would basically follow the same evolution in the early universe. Therefore, in addition to a nonthermal scalar, we can either have the lightest ν_R or all the three ν_R be nonthermal during neutrino genesis.

Nevertheless, three ν_R being out of equilibrium implies that their Yukawa couplings should all be small enough, where the CP-violating source could be suppressed. In this case, increasing the Yukawa coupling should be taken carefully since the right-handed neutrinos may reach thermal equilibrium towards the end of neutrino genesis, where the washout effect discussed in section 3.2 will readily dilute the ν_R asymmetries.

When the two heavier ν_R have larger Yukawa couplings such that they already reached thermal equilibrium at neutrino genesis, there would be a Yukawa coupling enhancement in the CP-violating source. In addition, large Yukawa couplings will open more detection channels to test the neutrinophilic scalar scenario.

In either case, it is helpful to estimate the maximal neutrino Yukawa coupling that can delay neutrino thermalization. Since right-handed neutrinos are gauge singlets, the evolution of ν_R is well determined by decay and inverse decay of the neutrinophilic scalar. In the SK-CTP formalism, the one-loop neutrino self-energy diagrams shown in Fig. 1 can also be used to determine the abundance of right-handed neutrinos. Given that the two-loop diagram shown in Fig. 3 determines the number asymmetry $n_\nu - n_{\bar{\nu}}$, we can neglect the small asymmetry $f_\alpha - \bar{f}_\alpha$ when calculating the time evolution of f_α from Fig. 1. Under this approximation, the Boltzmann equation usually suffices to capture the solution of f_α , which is easier to manage since the amplitudes of decay and inverse decay are obtained from tree-level diagrams. For consistent checks, we will still apply the KB equation of f_α . To this end, we first multiply $\text{sign}(p_0)$ on both sides of the KB equation given in Eq. (3.4), take the Dirac trace, and then integrate over p_0 .⁶ We arrive at

$$\begin{aligned} \frac{df_\alpha}{dt} &= \frac{1}{8\pi} \int dp_0 \text{sign}(p_0) \text{Tr} \left[i\mathcal{Y}_{\nu\alpha}^> i\mathcal{S}_{\nu\alpha}^< - i\mathcal{Y}_{\nu\alpha}^< i\mathcal{S}_{\nu\alpha}^> \right]_{1\text{-loop}} \\ &= \frac{|y_\alpha|^2 m_\phi^2}{32\pi p^2} \int_{m_\phi^2/(4p)}^\infty dp_\ell I(p_\ell, p), \end{aligned} \quad (3.26)$$

where the integration limit $p_\ell > m_\phi^2/(4p)$ reflects energy-momentum conservation $p_\phi^\mu = p_\ell^\mu + p^\mu$ in decay/inverse decay. The statistics function is given by

$$I(p_\ell, p) \equiv f_\phi^{\text{eq}}(p_\ell + p) [1 - f_\ell^{\text{eq}}(p_\ell)] - f_\alpha(p) [f_\phi^{\text{eq}}(p_\ell + p) + f_\ell^{\text{eq}}(p_\ell)], \quad (3.27)$$

where we have taken the thermal distribution functions for the scalar and leptons. Rearranging the above statistics function, we can check that it is equivalent to that from Boltzmann equation: $f_\phi^{\text{eq}}(1 - f_\ell^{\text{eq}})(1 - f_\alpha) - f_\ell^{\text{eq}} f_\alpha (1 + f_\phi^{\text{eq}})$. This confirms that the KB equation can derive the Boltzmann

⁶To avoid confusion, we should emphasize that this treatment is different from Eq. (3.10) and will not lead to a collision rate scaling as $f_\alpha - \bar{f}_\alpha$.

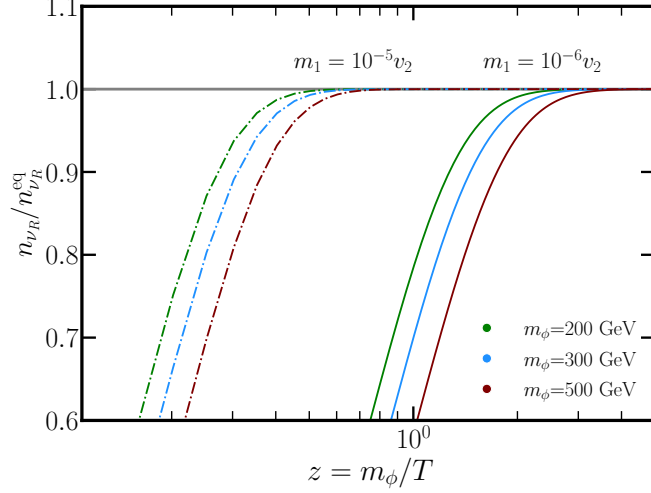


Figure 4. The evolution of ν_{R1} from ϕ decay and inverse decay, normalized to the thermal equilibrium limit. The benchmark point $m_1/v_2 = 10^{-6}$ (10^{-5}) typically corresponds to the situation where ν_{R1} thermalization occurs after (before) $T = m_\phi$. Here, we take the normal ordering for illustration, where m_1 corresponds to the lightest neutrino mass.

equation when the KB ansatz and quasiparticle approximation are applied [65].

For concreteness, we take $\alpha = 1$ to see the evolution of the neutrino number density normalized to the equilibrium limit:

$$n_{\nu_R}^{\text{eq}} = \int \frac{d^3p}{(2\pi)^3} \frac{1}{e^{p/T} + 1}. \quad (3.28)$$

We show in Fig. 4 the normalized neutrino number density in terms of the time variable $z \equiv m_\phi/T$. We choose two special values $m_1/v_2 = 10^{-6}, 10^{-5}$ to illustrate the moments when ν_{R1} reaches full thermal equilibrium. We see that $m_1/v_2 = 10^{-6}$ typically results in ν_R thermalization after $T = m_\phi$ while $m_1/v_2 = 10^{-5}$ leads to earlier thermalization unless the scalar mass becomes large. Nevertheless, forbidden neutrino genesis from a heavier scalar implies that there would be a longer period between the completion of neutrino genesis and sphaleron decoupling. This would still lead to a strong washout effect even if ν_R thermalization occurs after $T = m_\phi$.

If forbidden neutrino genesis completes before sphaleron decoupling due to ν_R thermalization, we should check whether the strong washout of ν_R asymmetries occurs. The thermalization moments shown in Fig. 4, together with the dilution exponent shown in Fig. 2, will provide such checks in the next section. In particular, avoiding the strong washout effect generally requires $m_\phi < 500$ GeV for a neutrino Yukawa coupling $|y| = 10^{-6}$.

3.5 Neutrino asymmetries

3.5.1 Three nonthermal neutrinos

We first consider the CP-violating source in the case of three nonthermal ν_R . We will work at leading order of $\delta f \equiv f - f^{\text{eq}}$ and neglect the quadratic correction $\delta f_\phi \delta f_{\nu_R}$ from both the nonthermal scalar and neutrinos. Therefore, for three nonthermal ν_R , we will take the thermal distribution for the scalar. We relegate the detailed calculations of the CP-violating rate to Appendix C. The final

result is rather simple and reads

$$\mathcal{S}_{\text{CP}} = \frac{\text{Im}(y_4)m_\phi^4}{256\pi^4(\tilde{m}_j^2 - \tilde{m}_i^2)} \int_0^\infty \frac{dp_\ell}{p_\ell} \int_{\frac{m_\phi^2}{4p_\ell} + p_\ell}^\infty dE_\phi \int_{\frac{m_\phi^2}{4p_\ell}}^\infty dq I(p_\ell, E_\phi, q), \quad (3.29)$$

where the statistics function gives

$$I(p_\ell, E_\phi, q) = \delta f_\beta(q)[f_\phi^{\text{eq}}(E_\phi) - f_\alpha(E_\phi - p_\ell)][f_\phi^{\text{eq}}(q + p_\ell) + f_\ell^{\text{eq}}(p_\ell)]. \quad (3.30)$$

Given Eqs. (3.18) and (3.25), we see that if the distribution functions for right-handed neutrinos are flavor universal, \mathcal{S}_{CP} would vanish after summing over neutrino flavors α, β , and hence the total CP asymmetry in the ν_R sector vanishes. However, it is generally not the case due to the flavor-dependent Yukawa couplings.

The statistics function given in Eq. (3.30) clearly dictates that no CP-violating source exists if all the particles are in thermal equilibrium. On the other hand, since the inner-loop scalar is heavier than the external leptons, the inner loop particles cannot go on-shell in vacuum due to the kinetic threshold. This is understood by the optical theorem in vacuum quantum field theory that the external leptons decay to the heavier scalar is kinetically forbidden. However, the thermal distributions of particles in the plasma open more energy-momentum conserved emission and absorption processes [66], with the transition probability weighted by these distributions. This can be simply seen if we drop the distribution functions of right-handed neutrinos in the inner loop, which amounts to neglecting the finite-density background of right-handed neutrinos, the CP-violating source \mathcal{S}_{CP} would vanish. This dependence on distribution functions from inner-loop particles demonstrates the very nature of forbidden leptogenesis.

From the result of $I(p_\ell, E_\phi, q)$, it is worth mentioning that the dependence of the distribution functions from the outer loop is linear in $f_\phi - f_\alpha$ and from the inner loop is linear in $f_\phi + f_\ell$. Such linear dependence is a consequence of calculating the two-loop amplitudes under the KB equation. It was previously found to be different from the quadratic dependence obtained by applying the finite-temperature time-ordered cutting rules to S -matrix amplitudes [6] unless the retarded/advanced cutting rules are properly used [20, 26, 67]. However, the calculation of forbidden leptogenesis via the S -matrix formalism embedded in the semi-classical Boltzmann equations can also lead to inconsistent conclusions. In section 4.1, we will make a comparison between the calculations of two-loop self-energy diagrams under the KB equation and of one-loop self-energy diagrams under the Boltzmann equation, pointing out that forbidden leptogenesis within the Boltzmann approach also suffers from the real-intermediate-subtraction issue [6, 29].

In the weak washout regime, we may neglect the washout rate such that the particle-number asymmetry stored in three right-handed Dirac neutrinos would simply read

$$Y_\nu = \sum_\alpha Y_{\nu R\alpha} = \int_{T_{\text{sph}}}^\infty \frac{\mathcal{S}_{\text{CP}}}{s_{\text{SM}} \mathcal{H} T} dT. \quad (3.31)$$

where the entropy density and the Hubble parameter are given by Eq. (3.2) and Eq. (3.13), respectively, and we have cut the temperature integration at the sphaleron decoupling moment $T_{\text{sph}} \approx 132 \text{ GeV}$.⁷ The right-hand side of Eq. (3.31) is a 4-dimensional integral, where the Monte Carlo

⁷The modification to the SM prediction of T_{sph} depends on the λ parameters given in the Higgs potential (2.1), which we assume to be small here for simplicity. We mention that a larger T_{sph} will reduce Y_ν , but will also suppress the washout effect.

| Patterns | (m_1, m_2, m_3) (meV) | $10^{16} \mathcal{S}_{\text{CP}} / \sin \delta_{\text{CP}}$ (eV ⁴) |
|-------------------------------|-------------------------|--|
| NO+ $m_{1,\text{max}}$ | (30.14, 31.36, 58.49) | 1.21 ($\langle \delta f_3 \rangle - \langle \delta f_2 \rangle$) |
| NO+ $10^{-3}m_{1,\text{max}}$ | (0.03, 8.65, 50.13) | 0.89 ($\langle \delta f_3 \rangle - \langle \delta f_2 \rangle$) |
| IO+ $m_{3,\text{max}}$ | (51.63, 52.35, 16.02) | -0.09 ($\langle \delta f_2 \rangle - \langle \delta f_3 \rangle$) |
| IO+ $10^{-3}m_{3,\text{max}}$ | (49.08, 49.84, 0.016) | $-9 \times 10^{-8} (\langle \delta f_2 \rangle - \langle \delta f_3 \rangle)$ |

Table 1. Behavior of \mathcal{S}_{CP} in terms of the neutrino mass spectrum and Dirac CP-violating phase δ_{CP} in the case of three nonthermal ν_R . Pattern NO+ $m_{1,\text{max}}$ (IO+ $m_{3,\text{max}}$) denotes the normal (inverted) ordering with a maximally allowed mass for the lightest neutrino, and NO+ $10^{-3}m_{1,\text{max}}$ (IO+ $10^{-3}m_{3,\text{max}}$) denotes the normal (inverted) ordering but with a smaller value for the lightest neutrino mass. The mass spectrum in NO (IO) gives $m_1 < m_2 < m_3$ ($m_3 < m_1 < m_2$), where δf_3 corresponds to the heaviest (lightest) neutrino. \mathcal{S}_{CP} is estimated via Eq. (3.32), and $v_2 = 1$ keV is chosen, which only affects the overall magnitude of \mathcal{S}_{CP} .

algorithm is sufficient to perform the numerical integration.

In Eq. (3.31), the dependence of Y_ν on the PMNS phase and the neutrino mass spectrum opens an avenue to test the minimal forbidden leptogenesis. Measurements of PMNS elements from neutrino oscillation in recent years have suggested some correlation between the sign of $\sin \delta_{\text{CP}}$ and the neutrino mass ordering [64]. In the normal ordering (NO), where $m_1 < m_2 < m_3$, the maximal CP violation with $\delta_{\text{CP}} = \pi/2$ is disfavored at 3σ level. In the inverted ordering (IO), where $m_3 < m_1 < m_2$, the maximal CP violation with $\delta_{\text{CP}} = 3\pi/2$ is favored by both the T2K [68, 69] and NO ν A [70] experiments. In addition, $0 < \delta_{\text{CP}} < \pi$ is disfavored in the IO pattern within the 3σ range of data. Based on Eq. (3.29), we will first analyze the dependence of the CP-violating source on δ_{CP} and the lightest neutrino mass, and then see how measurements of these observables can help to probe forbidden leptogenesis in the minimal scenario.

We take the data from NuFIT 6.0 [64]. We fix the mixing angles with their best-fit points, which do not deviate significantly between the NO and the IO, and take the two squared mass differences with their central values. We apply the upper bound on the sum of neutrino masses from Planck [59], with $\sum_i m_i < 0.12$ eV. For each ordering pattern, we take the lightest neutrino mass with a value approaching the upper bound and a much smaller one. We further estimate \mathcal{S}_{CP} by taking the maximal resonant enhancement from the muon Yukawa coupling.⁸ Let us define

$$\mathcal{S}_{\text{CP}} \equiv \frac{\text{Im}(y_4)}{8\pi^4 y_\mu^2} \langle f_\beta \rangle, \quad (3.32)$$

where $\langle \delta f_\beta \rangle$ is a dimensionful average of δf_β under the integration of Eq. (3.29). $\langle \delta f_\beta \rangle$ depends sensitively on the neutrino flavor β , but weakly on flavor α . Given this, we neglect f_α from Eq. (3.30) at the moment to estimate Eq. (3.32), but will include f_α at a later stage.

Following the above setup, we show in Tab. 1 the neutrino mass spectrum and \mathcal{S}_{CP} in four different patterns. In the pattern of NO+ $m_{1,\text{max}}$, the first two generations have similar masses and hence we expect $\langle \delta f_1 \rangle \approx \langle \delta f_2 \rangle$. However, the third generation has a larger mass, indicating a larger Yukawa coupling and hence $\langle \delta f_2 \rangle < \langle \delta f_3 \rangle < 0$. Therefore we see that $0 < \delta_{\text{CP}} < \pi$ will lead to a positive Y_B .

In pattern NO + $10^{-3}m_{1,\text{max}}$, the lightest neutrino mass m_1 is taken by $10^{-3} \times m_{1,\text{max}}$,

⁸This corresponds to $j = 2, i = 1$ in Eq. (3.29). Note that the result from $j = 1, i = 2$ is identical to $j = 2, i = 1$ since $\text{Im}[y_4(j = 1, i = 2)] = -\text{Im}[y_4(j = 2, i = 1)]$.

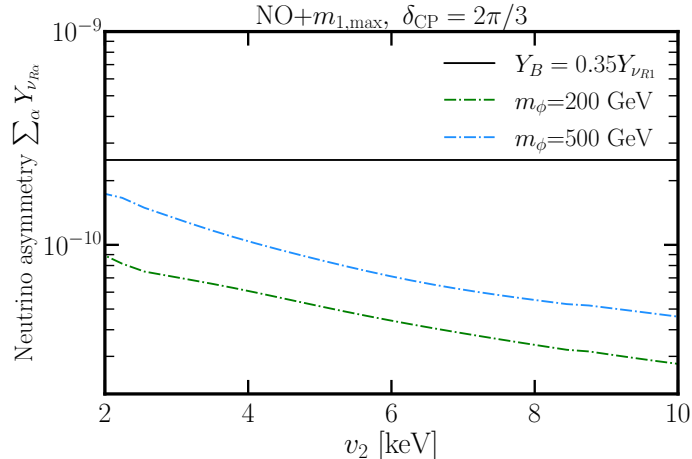


Figure 5. The total asymmetry in the case of three nonthermal ν_R . Pattern NO with a maximal value for the lightest neutrino mass $m_{1,\max} \approx 0.03$ eV is taken for illustration, where the Dirac CP-violating phase is fixed by $\delta_{\text{CP}} = 2\pi/3$.

which implies a much smaller Yukawa coupling for the lightest generation and hence a negligible contribution to \mathcal{S}_{CP} . In this case, however, the dominant contribution from the two heavier ν_R does not change significantly, so we still obtain a result similar to NO+ $m_{1,\max}$, where $0 < \delta_{\text{CP}} < \pi$ is responsible for a positive Y_B .

In pattern IO+ $m_{3,\max}$, the heavier two generations have similar masses and hence we expect $\langle \delta f_1 \rangle \approx \langle \delta f_2 \rangle$. Furthermore, due to a smaller mass for the lightest neutrino, we expect $\langle \delta f_3 \rangle < \langle \delta f_2 \rangle < 0$. It indicates that $\pi < \delta_{\text{CP}} < 2\pi$ will lead to a positive Y_B . While \mathcal{S}_{CP} in IO+ $m_{3,\max}$ has a prefactor smaller than from NO+ $m_{1,\max}$ by one order of magnitude, CP violation in the IO pattern could still be maximal with $\sin \delta_{\text{CP}} = -1$ and larger than in the NO pattern with $\sin \delta_{\text{CP}} = \mathcal{O}(0.1)$. Therefore, \mathcal{S}_{CP} from both NO+ $m_{1,\max}$ and IO+ $m_{3,\max}$ could be at the same order of magnitude. The crucial difference in these patterns is that the condition $Y_B > 0$ requires different signs of $\sin \delta_{\text{CP}}$, where $0 < \delta_{\text{CP}} < \pi$ in the NO and $\pi < \delta_{\text{CP}} < 2\pi$ in the IO will be selected. This is actually in line with the implication from current measurements. Therefore, both NO and IO with the lightest neutrino mass approaching its maximal value can predict a positive baryon asymmetry. However, such degeneracy would break down if the NO pattern with $\pi \leq \delta_{\text{CP}} \leq 2\pi$ is detected in upcoming measurements.⁹

In pattern IO + $10^{-3}m_{3,\max}$, we expect $\langle \delta f_1 \rangle \approx \langle \delta f_2 \rangle$ since the two heavier generations become quasi-degenerate in the limit of vanishing m_3 . Unlike pattern NO + $10^{-3}m_{1,\max}$, this quasi-degenerate mass leads to a much smaller \mathcal{S}_{CP} , which will essentially vanish in the limit of $m_3 = 0$.

Before the full numerical computation of Eq. (3.31), let us get a rough estimate of the parameter space for $Y_{\nu} \simeq 10^{-10}$. Following Eq. (3.29), we can generally write

$$Y_{\nu} \sim \text{Im}(y_4) \left(\frac{m_{\text{P}}}{m_{\phi}} \right) \int z^4 I(x_{\ell}, x_{\phi}, x_{\alpha}) dx_{\ell} dx_{\phi} dx_{\alpha} dz, \quad (3.33)$$

up to $\mathcal{O}(1)$ corrections. The dimensionless variables are defined as $x_{\ell} \equiv p_{\ell}/T$, $x_{\phi} \equiv p_{\phi}/T$, $x_{\alpha} \equiv$

⁹Actually, this pattern has already been hinted by the best-fit point of δ_{CP} from NuFIT (<http://www.nu-fit.org>). However the favored values of δ_{CP} in the NO by the T2K [68, 69] and NO ν A [70] experiments do not agree.

$p/T, z \equiv m_\phi/T$. Note that we have taken the maximal enhancement from the muon Yukawa coupling $y_\mu \approx 6 \times 10^{-4}$, and the 4-dimensional integration may reach $\mathcal{O}(1)$ for large $\delta f_\beta \sim 0.1$.¹⁰ Taking this $\mathcal{O}(1)$ estimate and assuming an electroweak scalar, we find that the order of magnitude for the neutrino Yukawa couplings should be larger than 10^{-7} to match $Y_\nu \simeq 10^{-10}$. Given Eq. (3.25), we have $\text{Im}(y_4) \sim U^4 m^4/v_2^4$, where U^4 denotes the estimate of the PMNS matrix elements at the quartic power, with $U^4 \sim 0.01$. It turns out that we need $m/v_2 \gtrsim 10^{-5}$ to produce $Y_\nu \simeq 10^{-10}$. However, Fig. 4 suggests that $m/v_2 \gtrsim 10^{-5}$ would lead to a large washout effect.

The above estimate is confirmed by the full numerical computation of Eq. (3.31), as shown in Fig. 5. In pattern NO+ $m_{1,\text{max}}$, we see that generating the observed baryon asymmetry Y_B requires $v_2 < 2$ keV, which corresponds to $m_1/v_2 > 10^{-5}$. This will introduce a large washout factor since ν_R thermalization occurs at $z < 1$, as shown in Fig. 2. We conclude that when all the three ν_R are out of equilibrium at $T \sim m_\phi$, forbidden leptogenesis can only generate a maximum of the ν_R asymmetry at $\mathcal{O}(10^{-11})$.

3.5.2 One nonthermal neutrino

When the two heavier ν_R have larger Yukawa couplings such that they have reached thermal equilibrium during leptogenesis, a net ν_R asymmetry will only be accumulated in the lightest ν_R sector. In this case, the nonthermal condition is provided by the scalar and the lightest right-handed neutrino. The calculation of the CP-violating source still comes from Fig. 3, with the inner right-handed neutrinos (scalar) being in thermal equilibrium (out of equilibrium). Following the general CP-violating source derived in Ref. [13], we arrive at

$$\mathcal{S}_{\text{CP}} = \frac{\text{Im}(y_4)m_\phi^4}{256\pi^4(\tilde{m}_j^2 - \tilde{m}_i^2)} \int_0^\infty \frac{dp_\ell}{p_\ell} \int_{\frac{m_\phi^2}{4p_\ell} + p_\ell}^\infty dE_\phi \int_{\frac{m_\phi^2}{4p_\ell} + p_\ell}^\infty dE'_\phi I(p_\ell, E_\phi, E'_\phi), \quad (3.34)$$

with E'_ϕ the energy from the inner-loop scalar. Different from Eq. (3.30), the statistics function now reads

$$I(p_\ell, E_\phi, E'_\phi) = f_\phi^{\text{eq}}(E_\phi) \delta f_\phi(E'_\phi) [f_{\nu_R}^{\text{eq}}(E'_\phi - p_\ell) + f_\ell^{\text{eq}}(p_\ell) - 1], \quad (3.35)$$

where $f_{\nu_R}^{\text{eq}}$ is the thermal distribution function for the two heavier ν_R , and $\delta f_\phi = f_\phi - f_\phi^{\text{eq}}$. Note that the dependence on flavor β disappears in the statistics function, but we still have $\sum_\beta \text{Im}(y_4) \neq 0$ since α is no longer a dummy index and is fixed to be the lightest neutrino flavor, where

$$Y_\nu = Y_{\nu_{R1}} = \int_{T_{\text{sph}}}^\infty \frac{\mathcal{S}_{\text{CP}}}{s_{\text{SM}} \mathcal{H} T} dT. \quad (3.36)$$

Analogously to Eq. (3.32), let us analyze the dependence on the PMNS phase and the neutrino mass spectrum. We now define

$$\mathcal{S}_{\text{CP}} \equiv \frac{\text{Im}(y_4)}{8\pi^4 y_\mu^2} \langle \delta f_\phi \rangle, \quad (3.37)$$

where $\langle \delta f_\phi \rangle$ ¹¹ is a dimensionful average of δf_ϕ under the 3-dimensional integration of Eq. (3.34).

¹⁰Typically, the integration over Bose-Einstein and Fermi-Dirac distributions can reach $\mathcal{O}(1)$, while the integration over z is dominated at $z = \mathcal{O}(1)$, corresponding to the epoch when leptogenesis culminates.

¹¹Note that $\langle \delta f_\phi \rangle < 0$ is expected since $f_{\nu_R}^{\text{eq}} + f_\ell^{\text{eq}} - 1 \leq 0$ and $\delta f_\phi > 0$ is caused by the scalar mass effect, as indicated by Eq. (3.39).

| Patterns | (m_1, m_2, m_3) (meV) | $10^{12} \mathcal{S}_{\text{CP}} / \sin \delta_{\text{CP}}$ (eV ⁴) |
|-----------------------------|-----------------------------------|--|
| NO with $m_1/v_2 = 10^{-6}$ | (10 ⁻³ , 8.65, 50.13) | 1.15 $ \langle \delta f_\phi \rangle $ |
| IO with $m_3/v_2 = 10^{-6}$ | (49.08, 49.84, 10 ⁻³) | 0.04 $ \langle \delta f_\phi \rangle $ |

Table 2. Behavior of \mathcal{S}_{CP} in the case of one nonthermal ν_R , where patterns NO+ $m_{1,\text{max}}$ and IO+ $m_{3,\text{max}}$ shown in Tab. 1 cannot realize forbidden neutrino genesis. \mathcal{S}_{CP} is estimated via Eq. (3.37) with $|\langle \delta f_\phi \rangle| = -\langle \delta f_\phi \rangle$, and $v_2 = 1$ eV is chosen.

We show in Tab. 2 the CP-violating rate in pattern NO (IO) with $m_1/v_2 = 10^{-6}$ ($m_3/v_2 = 10^{-6}$). Note that the patterns with $m_{1,\text{max}}$ and $m_{3,\text{max}}$ cannot realize neutrino genesis since the lightest ν_R must be out of equilibrium. In contrast to the case of three nonthermal ν_R , a positive Y_B requires $0 < \delta_{\text{CP}} < \pi$ in both NO and IO patterns. This is expected since the dependence of \mathcal{S}_{CP} on ν_R flavors now comes from $\text{Im}(y_4)$, which has the same dependence on δ_{CP} in both NO and IO patterns. Given that $0 < \delta_{\text{CP}} < \pi$ is disfavored in the IO pattern,¹² we conclude that only the NO pattern can realize forbidden neutrino genesis in the case of one nonthermal ν_R .

Comparing to the case of three nonthermal ν_R that features small Yukawa couplings, large Yukawa couplings from the two heavier ν_R in the case of one nonthermal ν_R will enhance the CP-violating source. Such an enhancement plays a significant role in compensating for the suppression from a quasi-thermal scalar, where δf_ϕ is small. In general, there is larger parameter space to realize forbidden neutrino genesis in the case of one nonthermal ν_R , depending on the scale of $|y_2|, |y_3|$. Here, we will consider a simple situation where both $|y_2|$ and $|y_3|$ are large enough to dominate the scalar evolution but small enough such that the resonant enhancement from soft-lepton resummation is valid.¹³ In this case, the evolution of the scalar under the KB (or equivalently Boltzmann) equation with collision rates from decay and inverse decay is given by [13]

$$\frac{\partial f_\phi}{\partial t} - \mathcal{H} p_\phi \frac{\partial f_\phi}{\partial p_\phi} = -\delta f_\phi \frac{|y_\alpha|^2 m_\phi^2 T}{8\pi E_\phi p_\phi} \ln \left(\frac{\cosh \left(\frac{E_\phi + p_\phi}{4T} \right)}{\cosh \left(\frac{E_\phi - p_\phi}{4T} \right)} \right), \quad (3.38)$$

where $p_\phi \equiv |\vec{p}_\phi|$, and α contains the two heavier ν_R flavors.

Similarly to Fig. 5, we first present the scale of v_2 that can induce a large ν_{R1} asymmetry, which is shown in the left panel of Fig. 6. We fix $m_1/v_2 = 10^{-6}$ to avoid the washout effect, and the integration of temperature is cut in the IR regime via $z = m_\phi/T_{\text{sph}}$. We see that $Y_{\nu_{R1}}$ at the order of Y_B typically requires $v_2 = \mathcal{O}(1)$ eV, which implies $|y_2| \sim |y_3| \sim 0.01$ for the two heavier ν_R . We see from the left panel that a lighter scalar results in a larger $Y_{\nu_{R1}}$ when v_2 is lower, but a heavier scalar leads to a larger $Y_{\nu_{R1}}$ when v_2 becomes higher. This can be explained by the behavior of δf_ϕ from Eq. (3.38), which has the structure

$$\frac{d\delta f_\phi}{dz} \sim -|y_\alpha|^2 \frac{M_P}{m_\phi} \delta f_\phi + \left| \frac{df_\phi^{\text{eq}}}{dz} \right|. \quad (3.39)$$

We can see that the mass effect in f_ϕ^{eq} drives the scalar into the out-of-equilibrium regime, which is the source for δf_ϕ . If there is no vacuum mass for the scalar before gauge symmetry breaking, i.e.,

¹²Both the T2K and NO ν A experiments are consistent with $\pi < \delta_{\text{CP}} < 2\pi$ in the IO pattern within 3σ level.

¹³We will demonstrate this point in Appendix B.

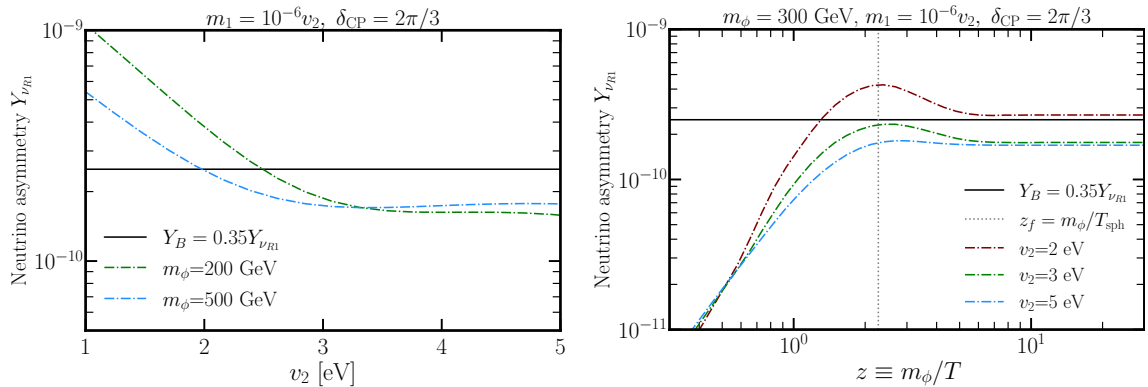


Figure 6. Left: the magnitude of the ν_{R1} asymmetry $Y_{\nu_{R1}}$ in terms of v_2 . Right: the evolution of $Y_{\nu_{R1}}$ from $m_\phi = 300$ GeV, where the vertical dotted line denotes the epoch of sphaleron decoupling. Only the NO pattern works to generate a positive Y_B , where the Dirac CP-violating phase is fixed by $\delta_{CP} = 2\pi/3$.

$\mu_2 \ll v_1 \approx 246$ GeV, we would obtain $df_\phi^{\text{eq}}/dz = 0$ and $\delta f_\phi = 0$ will be maintained from an initial equilibrium state. The first term on the right-hand side can be regarded as the exponential dilution for δf_ϕ . For larger v_2 , the Yukawa couplings become smaller and hence the dilution will become exponentially suppressed, increasing δf_ϕ thereby. Note that this effect would be stronger for larger scalar masses due to the ratio M_P/m_ϕ . The resulting enhancement of δf_ϕ can compete with the power suppression from $\text{Im}(y_4)$, potentially allowing a larger $Y_{\nu_{R1}}$ for higher v_2 . This explains the tendency in the left panel of Fig. 6 for $m_\phi = 500$ GeV. It implies that a larger v_2 (smaller neutrino Yukawa couplings) does not always lead to $Y_{\nu_{R1}}$ suppression.

To see the evolution of $Y_{\nu_{R1}}$ in terms of the time variable $z \equiv m_\phi/T$, we show in the right panel of Fig. 6 with a benchmark scalar mass: $m_\phi=300$ GeV. The ratio $m_1/v_2 = 10^{-6}$ is fixed to avoid the strong washout effect, and this can be justified from Fig. 4, where ν_R thermalization occurs after sphaleron decoupling. We set an initial condition at $z_i = 10^{-3}$ with a thermal scalar and two thermal ν_R . In general, neutrino genesis culminates at $z \sim 3-5$ due to Boltzmann suppression in the statistics function $I(p_\ell, E_\phi, E'_\phi)$. However, a light scalar can lead to earlier completion of neutrino genesis due to sphaleron decoupling. In such a situation, neutrino genesis ends before a final stable value of $Y_{\nu_{R1}}$ is reached. This can be seen through the vertical dotted line ($z_f = m_\phi/T_{\text{sph}}$) in the right panel for $m_\phi = 300$ GeV.

We conclude that an electroweak scalar is able to realize forbidden neutrino genesis, where the neutrinophilic vacuum expectation value resides in the eV scale. Forbidden neutrino genesis works to explain the BAU only in the NO pattern with $\sin \delta_{CP} > 0$, where the lightest ν_R is out of equilibrium during neutrino genesis. This scenario is highly falsifiable in upcoming neutrino oscillation experiments. In particular, if $\pi < \delta_{CP} < 2\pi$ turns out to be the truth for an NO neutrino mass spectrum: $m_1 \ll m_2 < m_3$, it would be able to exclude the minimal neutrinophilic scalar scenario with $v_2 = \mathcal{O}(1)$ eV, as the framework can readily induce a large negative baryon asymmetry in the early universe via forbidden neutrino genesis.

4 Discussions

4.1 Comparison with the Boltzmann equation

Forbidden leptogenesis via lepton-number conserving interactions was previously considered in Refs. [62, 67], where the Boltzmann equation was used and the kinetic phase was derived from

the retarded/advanced cutting rules in the one-loop self-energy diagrams. Moreover, the nonthermal condition that realized forbidden leptogenesis was only provided by one ν_R flavor. This is qualitatively inconsistent with the results obtained from the SK-CTP formalism followed by the KB equation [13], which, as also shown in previous sections, points out that additional nonthermal conditions must be provided either by the scalar or by the other ν_R flavors from the inner loop of Fig. 3.

The reason behind such inconsistency is that the evolution of CP asymmetries generated by the pure plasma effect was determined by the Boltzmann equation in Refs. [62, 67], where the real-intermediate-state subtraction [29] was not taken properly. It is known that if the on-shell scattering effect in the Boltzmann equation was not included consistently, CP asymmetries can still be generated even in thermal equilibrium. This is inconsistent with unitarity and the CPT theorem [6]. In Refs. [62, 67], only the decay and inverse decay processes were included in the Boltzmann equation, which neglected the on-shell scattering process that has a canceling effect on the CP asymmetry induced by decay/inverse decay.

Real-intermediate-state subtraction should also be taken into account in forbidden leptogenesis, which, however, can be circumvented in the SK-CTP formalism in a straightforward way [13, 18]. To see this, let us recall the five contributions to the CP-violating source \mathcal{S}_{CP} , which are parameterized by functions \mathcal{I}_i and \mathcal{J}_i given in Appendix C. The contributions of decay and inverse decay arise from $\mathcal{I}_{1,3,4,5}$ and $\mathcal{J}_{1,3,4,5}$, while the on-shell scattering contributions would arise from \mathcal{I}_2 (Eq. (C.5)) and \mathcal{J}_2 (Eq. (C.24)) when one of the resummed retarded lepton propagators $\mathcal{G}_{\ell_i}^R$ or $\mathcal{G}_{\ell_j}^R$ goes on-shell. Such on-shell scattering contributions ensure the appearance of the *thermal-criterion* function \mathcal{TC} given in Eq. (C.11), which guarantees no CP asymmetry in thermal equilibrium (Eq. (C.13)) and hence consistency with unitarity and the CPT theorem.

It is not clear yet whether one can start from the Boltzmann equation with one-loop self-energy amplitudes to evaluate forbidden leptogenesis. The reason behind is that there is no simple principle to write down the propagators in the one-loop self-energy diagrams built in the Boltzmann collision rates. In particular, inserting the thermal mass into fermion Feynman propagators is not justified theoretically. Cutting rules, or circling rules at finite-temperature field theory [71, 72] provide a possibility for studying purely plasma-induced effects within the Boltzmann equation, but are as technically nontrivial as the calculation of the KB collision rates in the SK-CTP formalism. Finding a simple correspondence between the two approaches deserves further considerations.

4.2 Phenomenology

The minimal neutrinophilic scalar scenario introduces several new-physics effects that could be observed in cosmology, low-energy flavor physics and colliders. In this section, we will briefly discuss some of the potential signals that follow the realization of forbidden neutrinogenesis.

In cosmology, since three ν_R are the right-handed Dirac counterparts of the SM ν_L , they contribute as extra radiation to the expansion of the universe, affecting processes during the big-bang nucleosynthesis (BBN) and cosmic microwave background (CMB) epochs. After neutrino decoupling, the effect of the accelerated cosmic expansion due to relativistic ν_R is parameterized by the effective neutrino number:

$$\Delta N_{\text{eff}} = \sum_{\alpha} \Delta N_{\alpha, \text{eff}} \equiv \sum_{\alpha} \frac{\rho_{\alpha}}{\rho_{\nu}^{\text{SM}}}, \quad (4.1)$$

where ρ_{α} is the energy density of $\nu_{R\alpha}$, and ρ_{ν}^{SM} denotes the energy density of one-generation ν_L

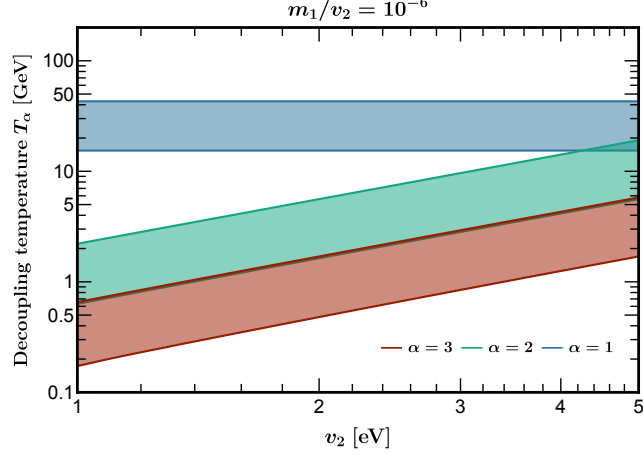


Figure 7. The decoupling temperatures of the three ν_R flavors in the NO pattern, where $\alpha = 3(1)$ corresponds to the heaviest (lightest) ν_R . The upper (lower) boundary for each α corresponds to $m_\phi = 500$ (200) GeV. We set $m_1/v_2 = 10^{-6}$ such that T_1 is independent of v_2 .

in the SM:

$$\rho_\nu^{\text{SM}} = \frac{7}{4} \frac{\pi^2}{30} T_\nu^4, \quad (4.2)$$

with $T_\nu \approx (4/11)^{1/3} T$ after neutrino decoupling.

Thermalized right-handed neutrinos, as predicted in the case of one nonthermal ν_R , will give significant contributions to ΔN_{eff} . Using Eq. (4.1) and entropy conservation, one can easily derive

$$\Delta N_{\alpha, \text{eff}} \approx 0.027 \left(\frac{106.75}{g_s(T_\alpha)} \right)^{4/3} g_\alpha, \quad (4.3)$$

for thermalized ν_R of flavor α . Here, $g_s(T_\alpha)$ is the SM effective degrees of freedom at the $\nu_{R\alpha}$ decoupling temperature T_α , and we have taken a reference point $g_s = 106.75$ from relativistic SM species at $T = \mathcal{O}(100)$ GeV. $g_\alpha = 2 \times 7/8$ is the effective spin degrees of freedom for $\nu_{R\alpha}$.

As elaborated in section 3, only the case of one nonthermal ν_R can realize forbidden neutrino-genesis to explain the BAU, where the NO pattern with $0 < \delta_{\text{CP}} < \pi$ is favored. In this case, the two heavier ν_R flavors have already reached thermal equilibrium at the neutrino-genesis epoch, while the lightest ν_R flavor will also establish thermalization after sphaleron decoupling. Nevertheless, the late-time evolution is not the same for the three ν_R . Due to the large Yukawa couplings ($|y_2| \sim |y_3| \sim 0.01$), right-handed neutrino scattering with charged leptons can maintain thermal equilibrium at $T \ll m_\phi$, and thermal equilibrium with ν_L could persist even after $T = \mathcal{O}(1)$ GeV. For the lightest ν_R , the much smaller Yukawa coupling ($|y_1| \sim 10^{-6}$) renders a suppressed four-fermion scattering rate such that left-right neutrino scattering will not maintain the equilibrium condition. Instead, nonrelativistic scalar decay and inverse decay $\phi \rightleftharpoons \ell + \bar{\nu}_R$ will determine the decoupling temperature of the lightest ν_R .

To determine the decoupling temperature T_α for ν_{R2} and ν_{R3} , we assume the neutral scalar boson H is the lightest one in the neutrinophilic scalar doublet, and focus on the t -channel $\nu_R +$

$\bar{\nu}_R \rightleftharpoons \nu_L + \bar{\nu}_L$ mediated by H . The annihilation cross section reads

$$\sigma_{\nu_R \bar{\nu}_R \rightarrow \nu_L \bar{\nu}_L} = \frac{m_i^2 m_j^2 s}{24\pi (m_H v_2)^4}, \quad (4.4)$$

where \sqrt{s} is the center-of-mass energy and the physical mass m_H is given in Eq. (2.13). The appearance of the two heavier neutrino masses m_i, m_j results from the application of Eq. (3.24). We substitute the annihilation cross section into the Boltzmann equation and obtain the thermally averaged annihilation rate [73]:

$$\langle \sigma v n \rangle \equiv \frac{T}{32\pi^4 n_{\nu_R}^{\text{eq}}} \int_0^\infty ds \sigma_{\nu_R \bar{\nu}_R \rightarrow \nu_L \bar{\nu}_L} s^{3/2} K_1(\sqrt{s}/T), \quad (4.5)$$

where K_1 is the modified Bessel function of the first kind, and $n_{\nu_R}^{\text{eq}}$ is the number density of thermalized ν_R . For the decoupling temperature of the lightest ν_R , we again concentrate on the neutral scalar boson H with the decay rate

$$\Gamma_{H \rightarrow \nu_L \bar{\nu}_R} = \frac{m_1^2}{16\pi v_2^2} m_H, \quad (4.6)$$

and with the nonrelativistic number density

$$n_H^{\text{eq}} = \left(\frac{m_H T}{2\pi} \right)^{3/2} e^{-m_H/T}. \quad (4.7)$$

We determine the decoupling temperatures T_i via¹⁴

$$\mathcal{H} = \langle \sigma v n \rangle, \quad \text{for } T_2, T_3, \quad (4.8)$$

$$n_{\nu_R}^{\text{eq}} \mathcal{H} = n_H^{\text{eq}} \Gamma_{H \rightarrow \bar{\nu}_L \nu_R}, \quad \text{for } T_1. \quad (4.9)$$

Motivated by the realization of forbidden neutrino genesis in the case of one nonthermal ν_R , we choose the parameter set: $v_2 = [1, 5]$ eV, $m_1/v_2 = 10^{-6}$ and $m_\phi = 200, 500$ GeV, and show the decoupling temperatures in Fig. 7. At the lower $m_H \cdot v_2$ end, i.e., $m_H = 200$ GeV and $v_2 = 1$ eV, the decoupling temperatures T_i are found to be around 170, 630, 1540 MeV, respectively. This amounts to $\Delta N_{\text{eff}} \approx 0.377$, which is larger than the current Planck bound [59]: $\Delta N_{\text{eff}} < 0.285$. At the higher $m_H \cdot v_2$ end, with $m_H = 500$ GeV and $v_2 = 5$ eV, on the other hand, the decoupling temperatures are found to be 5.8, 19, 43 GeV, respectively, giving rise to $\Delta N_{\text{eff}} \approx 0.186$. This lower value will be covered by future sensitivity from *e.g.*, the Simons Observatory experiment [74]. Therefore, cosmic measurements of N_{eff} will provide a robust test for forbidden neutrino genesis in the neutrinophilic scalar scenario.

Next, let us consider the signatures from low-energy flavor physics. It has been noticed that one of the most sensitive probes for the neutrinophilic scalar scenario comes from lepton-flavor violating transitions [75], particular in $\mu \rightarrow e\gamma$, $\mu \rightarrow 3e$, and $\mu \rightarrow e$ in nuclei. Current bounds

¹⁴While we do not intend to calculate the precise T_α here, we should mention that this treatment, together with Eq. (4.5) that is valid by taking the approximation of the Boltzmann distribution, leads to some uncertainty in the T_α calculation. Nevertheless, Eq. (4.3) suggests that a precise T_α only becomes significant around the QCD phase transition $T_{\text{QCD}} \sim 200$ MeV.

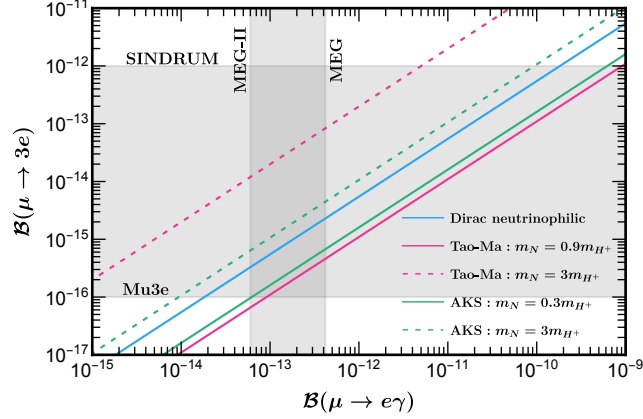


Figure 8. The correlation between the branching ratios of $\mathcal{B}(\mu \rightarrow 3e)$ and $\mathcal{B}(\mu \rightarrow e\gamma)$ in the Dirac neutrinophilic scalar scenario and some typical models with Majorana neutrinos. Current and future bounds are shown in shaded regions. The predictions from the Tao-Ma [82, 83] and the AKS [84, 85] models are shown with different mass ratios between the heavy Majorana neutrinos and charged scalar bosons, where order-one Yukawa couplings are assumed.

exclude the charged-scalar mass below 250 GeV for $v_2 = 1$ eV.¹⁵ Given that future sensitivities are forecast to increase by one to several orders of magnitude, such as the COMET experiment from J-PARC [76], MEG-II [77] and Mu3e [78], we expect that an electroweak neutrinophilic scalar with $v_2 = \mathcal{O}(1)$ eV can be fully tested. Moreover, the new-physics effects on these lepton-flavor violating transitions are correlated. Taking $\mu \rightarrow e\gamma$ and $\mu \rightarrow 3e$ for example, we have the branching ratios [75, 79]:

$$\frac{\mathcal{B}(\mu \rightarrow 3e)}{\mathcal{B}(\mu \rightarrow e\gamma)} \approx \frac{\alpha_{\text{EM}}}{36\pi} \left[24 \ln \left(\frac{m_\mu}{m_e} \right) - 43 \right], \quad (4.10)$$

where the approximation is valid in the regime $v_2 \gtrsim 1$ eV and takes into account the fact that charged leptons and Dirac neutrinos are much lighter than the charged scalar bosons. It is worth mentioning that in scenarios with heavy right-handed (Majorana) neutrinos coupling to scalar doublets, there could also be simple correlations between $\mu \rightarrow e\gamma$ and $\mu \rightarrow 3e$, such as the supersymmetric low-scale seesaw model [80, 81], the Tao-Ma scotogenic model [82, 83] and the AKS model [84, 85]. Unlike the minimal neutrinophilic scalar scenario with Dirac neutrinos, the correlations induced by these scenarios usually depend on additional Yukawa couplings and on the mass spectrum between the heavy Majorana neutrinos and the charged scalar bosons [86–89].

We show in Fig. 8 the correlation between $\mathcal{B}(\mu \rightarrow 3e)$ and $\mathcal{B}(\mu \rightarrow e\gamma)$, with the current (future) bounds of $\mu \rightarrow e\gamma$ from MEG [90] (MEG-II [77]) and of $\mu \rightarrow 3e$ from SINDRUM [91] (Mu3e [78]). As a comparison with the Dirac neutrinophilic scalar scenario, we also show the predictions from the Tao-Ma model and the AKS model with different mass ratios (m_N/m_{H^+}) between the heavy Majorana neutrinos and the charged scalar bosons. Notice that these predictions usually depend on additional Yukawa couplings, so we take order-one Yukawa couplings for illustration. It is seen that the predicted correlation line from the Dirac neutrinophilic scalar scenario lies between the two exemplary mass ratios in the Tao-Ma model and the AKS model. It implies that there exists certain degeneracy among these models in some parameter space, but such

¹⁵We mention that the charged-scalar mass given in Eq. (2.13) can be larger than the mass (μ_2) used in neutrino genesis before gauge symmetry breaking.

degeneracy can usually be removed via complementary probes.

In the Dirac neutrinophilic scalar scenario, the branching ratios of $\mu \rightarrow e\gamma$ and $\mu \rightarrow 3e$ depend on the product of m_{H^\pm} and v_2 [75, 79]. With increased sensitivities from the future MEG-II experiment on $\mu \rightarrow e\gamma$ and from the future Mu3e experiment on $\mu \rightarrow 3e$, we find that the correlated region that can be probed simultaneously by MEG-II and Mu3e is induced by $m_{H^\pm} \cdot v_2 = [332, 540]$ GeV · eV. For example, a charged-scalar mass at 300 GeV with $v_2 = 1.8$ eV can be probed via the correlated $\mu \rightarrow e\gamma$ and $\mu \rightarrow 3e$. This region covers the parameter space that can realize forbidden neutrinogenesis presented in section 3.5.2. The simultaneous observation of $\mu \rightarrow 3e$ and $\mu \rightarrow e\gamma$ in the future would provide an interesting indication of such a minimal neutrinophilic scalar scenario that can explain the BAU and neutrino masses.

Finally, we would like to comment on collider detection. For the minimal neutrinophilic scalar scenario that can realize the forbidden neutrinogenesis, there are several collider detection channels for the scalar bosons. For electroweak charged-scalar bosons, gauge interactions allow sizable cross sections from Drell-Yan production: $pp \rightarrow Z^*/\gamma^* \rightarrow H^+H^-$ at the LHC [92, 93], which is followed by prompt decay $H^\pm \rightarrow \ell^\pm + \nu_R$ due to large neutrino Yukawa couplings. Mono-lepton signals can arise from production of neutral and charged scalars, e.g., $pp \rightarrow W^{\pm*} \rightarrow H^\pm A$ [94, 95] followed by $H^\pm \rightarrow \ell^\pm + \nu_R$ and $A \rightarrow \nu_L + \bar{\nu}_R$. Purely neutral-scalar production can be constructed via $pp \rightarrow Z^* \rightarrow HA$, which, however, will be mostly followed by prompt decay to neutrinos, again due to large neutrino Yukawa couplings. Future lepton colliders, such as the Compact Linear Collider [96, 97], the International Linear Collider [98, 99] and the muon collider [100, 101] will also be useful to produce these new scalars. In particular, the mono-photon channel from initial-state radiation $e^+e^- \rightarrow Z^* \rightarrow HA(\rightarrow \text{missing energy}) + \gamma$ can provide an interesting avenue for purely neutral-scalar production, where the missing four-momentum can be calculated by using the photon energy and the photon polar angle [102, 103].

It has been a haunting concern to test leptogenesis at colliders, where generally no smoking-gun signal can be uniquely induced from leptogenesis. This situation would become worse if leptogenesis is realized by new physics with flavored scalars, since the indication of the BAU origin requires confirmation of the scalar family. Here, we would like to emphasize an *inverse perspective* of forbidden leptogenesis in motivating collider detection: if some new particle is detected at colliders, can this particle be ready to resolve the BAU problem? As elaborated in this paper, the BAU origin can be explained if there is an electroweak neutrinophilic scalar minimally introduced beyond the SM. While the collider signals mentioned above may not be the unique smoking-gun, they provide a simple indication that the BAU can already be attributed to such minimal new physics. This is different from flavored-scalar leptogenesis [11, 104–106], where more delicate collider confirmation is needed.

5 Conclusion

Plasma effects via soft-lepton resummation exhibit a resonant enhancement in generation of finite-temperature CP asymmetries, which can reach $\mathcal{O}(10^8)$ from quasi-degenerate lepton thermal masses. The enhancement is predicted within the SM and does not require vacuum mass degeneracy. Applying this kind of forbidden leptogenesis to the neutrinophilic scalar scenario in the SK-CTP formalism, we have elaborated that the minimal framework for the Dirac neutrino mass origin can further explain the BAU problem, where the scalar and one right-handed neutrino provide the nonthermal condition during neutrinogenesis.

The CP-violating source for forbidden neutrinogenesis in the minimal scenario comes directly from neutrino mixing. The Dirac CP-violating phase (δ_{CP}) in the PMNS matrix then determines the

sign of the baryon asymmetry. We find that the BAU explanation only favors the normal-ordering neutrino mass spectrum, where δ_{CP} should be in $(0, \pi)$ and the lightest neutrino is predicted to have a much smaller mass $m_1 \ll m_2 \approx m_3/6$. The connection between high-temperature leptogenesis and low-energy CP violation makes this scenario readily testable via upcoming measurements in neutrino oscillation experiments. In particular, either the inverted or normal ordering with $m_1 \ll m_2$ and $\pi < \delta_{\text{CP}} < 2\pi$ is able to exclude the minimal scenario with an electroweak scalar and an eV-scale vacuum expectation value, since the framework would generate a large negative baryon asymmetry in the early universe. On the other hand, forbidden leptogenesis cannot be realized in the minimal scenario if $m_1 \sim m_2$ is confirmed.

BBN and CMB measurements of N_{eff} in cosmology and the correlation between lepton-flavor violating transitions provide complementary probes of the minimal scenario, and will fully cover the parameter space for forbidden leptogenesis with forecast experimental sensitivities. Finally, the electroweak scalar accessible at colliders also provides another way to justify if the BAU problem can be already attributed to such minimal new physics.

The detailed calculation presented in this work also helps to understand the behavior of SM thermal leptons, with the aim of exploiting the maximal role of particles at finite temperatures. It allows stronger connections among complementary probes, minimizing the particle content in realizing leptogenesis.

Acknowledgements

We would like to thank Kei Yagyu for helpful discussions on the collider phenomenology of leptophilic scalars. This project is supported by JSPS Grant-in-Aid for JSPS Research Fellows No. 24KF0060. SK is also supported in part by Grants-in-Aid for Scientific Research(KAKENHI) Nos. 23K17691 and 20H00160.

A Propagators in the SK-CTP formalism

In the CTP formalism, if the system is close to thermal equilibrium, the free fermion propagators in a spatially homogeneous plasma can be formulated by

$$i\mathcal{S}^<(p) = -2\pi\delta(p^2 - m^2)(\not{p} + m) [\theta(p_0)f(p_0) - \theta(-p_0)(1 - \bar{f}(-p_0))], \quad (\text{A.1})$$

$$i\mathcal{S}^>(p) = -2\pi\delta(p^2 - m^2)(\not{p} + m) [-\theta(p_0)(1 - f(p_0) + \theta(-p_0)\bar{f}(-p_0))], \quad (\text{A.2})$$

$$i\mathcal{S}^T(p) = \frac{i(\not{p} + m)}{p^2 - m^2 + i\epsilon} - 2\pi\delta(p^2 - m^2)(\not{p} + m) [\theta(p_0)f(p_0) + \theta(-p_0)\bar{f}(-p_0)], \quad (\text{A.3})$$

$$i\mathcal{S}^{\bar{T}}(p) = -\frac{i(\not{p} + m)}{p^2 - m^2 - i\epsilon} - 2\pi\delta(p^2 - m^2)(\not{p} + m) [\theta(p_0)f(p_0) + \theta(-p_0)\bar{f}(-p_0)], \quad (\text{A.4})$$

and for scalar bosons,

$$iG^<(p) = 2\pi\delta(p^2 - m^2) [\theta(p_0)f(p_0) + \theta(-p_0)(1 + \bar{f}(-p_0))], \quad (\text{A.5})$$

$$iG^>(p) = 2\pi\delta(p^2 - m^2) [\theta(p_0)(1 + f(p_0)) + \theta(-p_0)\bar{f}(-p_0)], \quad (\text{A.6})$$

$$iG^T(p) = \frac{i}{p^2 - m^2 + i\epsilon} + 2\pi\delta(p^2 - m^2) [\theta(p_0)f(p_0) + \theta(-p_0)\bar{f}(-p_0)], \quad (\text{A.7})$$

$$iG^{\bar{T}}(p) = -\frac{i}{p^2 - m^2 - i\epsilon} + 2\pi\delta(p^2 - m^2) [\theta(p_0)f(p_0) + \theta(-p_0)\bar{f}(-p_0)], \quad (\text{A.8})$$

where \leq represent the Wightman functions and $T(\bar{T})$ the (anti) time-ordered propagators. $\theta(x)$ denotes the Heaviside step function. The above formulation is based on the KB ansatz in the quasi-particle approximation, which is a justified approximation in a close-to-equilibrium plasma. See *e.g.* Refs. [16, 60, 61]. Under this approximation, f, \bar{f} are regarded as the distribution functions of particles and antiparticles. In thermal equilibrium, we have

$$f^{\text{eq}}(p_0) = \bar{f}^{\text{eq}}(p_0) = \frac{1}{e^{p_0/T} \pm 1} \quad (\text{A.9})$$

for fermions (+) and bosons (-). Besides, the Kubo–Martin–Schwinger (KMS) relations hold:

$$\mathcal{G}^>(p) = -e^{p_0/T} \mathcal{G}^<(p), \quad G^>(p) = e^{p_0/T} G^<(p). \quad (\text{A.10})$$

In general, for a system far away from thermal equilibrium, the above formulation could fail to describe the dynamics and evolution [107, 108]. Fortunately, for most leptogenesis scenarios, the system is close to thermal equilibrium. This is also the case in forbidden neutrino genesis, since the dominant CP-asymmetry generation culminates at $0.1 \lesssim T/m_\phi \lesssim 1$, when both the scalar and right-handed neutrinos are close to thermal equilibrium.

B Soft-lepton resummation in Hard-Thermal-Loop approximation

At high temperatures, a (nearly) massless particle propagating in a thermal plasma will receive significant correction from the plasma if the propagation momentum is lower than the plasma temperature. An intuitive way to see the importance is to consider a massless propagator $1/p^2$, which can suffer from IR divergence when $p \rightarrow 0$. However, one-loop self-energy diagrams at finite temperatures can give $g^2 T^2$ correction to the dispersion relation, where g denotes a generic coupling in the theory. It implies that soft-momentum propagation at $p \sim gT$ should be taken properly as the IR enhancement will appear at $p \sim gT$ instead of $p = 0$. A technique to properly resolve this soft-momentum propagation at finite temperatures is the so-called Hard-Thermal-Loop (HTL) resummation [109–113]. In the HTL approximation, one-loop self-energy amplitudes are calculated by treating the external momentum at soft scale gT while taking the loop momentum at hard scale T . This has been implemented in soft-lepton resummation when we calculate the CP-violating rate from Fig. 3.

The resummed Wightman functions for SM leptons appeared in Eqs. (3.19)-(3.20) can be

expressed in terms of the resummed retarded $\R and advanced $\A propagators:

$$\$^<(p) = -f(p_0) \left[\$^R(p) - \$^A(p) \right], \quad (\text{B.1})$$

$$\$^>(p) = [1 - f(p_0)] \left[\$^R(p) - \$^A(p) \right], \quad (\text{B.2})$$

with the following relations

$$\$^T - \$^{\bar{T}} = \$^R + \$^A, \quad \$^> - \$^< = \$^R - \$^A. \quad (\text{B.3})$$

The resummed retarded propagator reads [114]

$$\$^R(p) = \frac{(1+a)\not{p} + b\not{\psi}}{[(1+a)p_0 + b]^2 - [(1+a)|\vec{p}|]^2} \equiv \sum_{\pm} \frac{1}{\text{Re}\Delta_{\pm} + i\text{Im}\Delta_{\pm}} P_{\pm}, \quad (\text{B.4})$$

where u_{μ} is the four-velocity of the plasma normalized by $u_{\mu}u^{\mu} = 1$ with $u_{\mu} = (1, 0, 0, 0)$ in the rest frame. Note that the resummed advanced propagator can be obtained from retarded propagator via $a, b \rightarrow a^*, b^*$. The dispersion relation and the thermal width of leptons are determined by the real and imaginary parts, respectively:

$$\text{Re}\Delta_{\pm}(p) \equiv (1 + \text{Re}a)(p_0 \pm |\vec{p}|) + \text{Re}b, \quad (\text{B.5})$$

$$\text{Im}\Delta_{\pm}(p) \equiv \text{Im}a(p_0 \pm |\vec{p}|) + \text{Im}b, \quad (\text{B.6})$$

and P_{\pm} denotes the decomposition of helicity eigenstates [115]

$$P_{\pm} \equiv \frac{\gamma^0 \pm \vec{e}_p \cdot \vec{\gamma}}{2}, \quad (\text{B.7})$$

with $\vec{e}_p \equiv \vec{p}/|\vec{p}|$.

For thermal particles with vacuum masses much smaller than the plasma temperature, the real coefficients $\text{Re}a, \text{Re}b$ can be analytically derived in the HTL approximation:

$$\text{Re}a_i = \frac{\tilde{m}_i^2}{|\vec{p}|^2} \left[1 + \frac{p_0}{2|\vec{p}|} \ln \left(\frac{p_0 - |\vec{p}|}{p_0 + |\vec{p}|} \right) \right], \quad (\text{B.8})$$

$$\text{Re}b_i = -\frac{\tilde{m}_i^2}{|\vec{p}|} \left[\frac{p_0}{|\vec{p}|} - \frac{1}{2} \left(1 - \frac{p_0^2}{|\vec{p}|^2} \right) \ln \left(\frac{p_0 - |\vec{p}|}{p_0 + |\vec{p}|} \right) \right], \quad (\text{B.9})$$

where \tilde{m} denotes the lepton thermal mass in the SM:

$$\tilde{m}_i^2 = \left(\frac{3}{32}g_2^2 + \frac{1}{32}g_1^2 + \frac{1}{16}y_{\ell_i}^2 \right) T^2, \quad (\text{B.10})$$

with g_2, g_1 the $SU(2)_L$ and $U(1)_Y$ gauge couplings, and y_{ℓ_i} the charged-lepton Yukawa couplings. To understand why \tilde{m}_i works as the effective mass, we express the pole $\text{Re}\Delta_- = 0$ as:

$$p_0 - |\vec{p}| = -\frac{\text{Re}b_i}{1 + \text{Re}a_i} \approx \frac{\tilde{m}_i^2}{|\vec{p}|} = \frac{m_{\text{eff}}^2}{p_0 + |\vec{p}|} \sim \frac{m_{\text{eff}}^2}{|\vec{p}|}, \quad (\text{B.11})$$

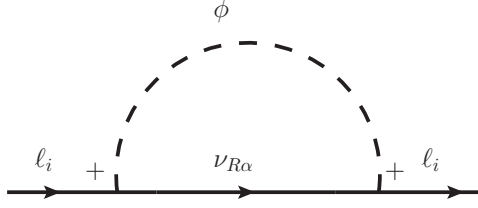


Figure 9. The new-physics contribution from Eq. (2.2) to lepton thermal masses, which comes from the real part of the time-ordered amplitude $\text{Re}\Sigma_\ell^{++} \equiv \text{Re}\Sigma_\ell^T$.

where the first approximation is obtained by taking $1 + \text{Re}a_i = \mathcal{O}(1)$ and using the leading-order relation $p_0/|\vec{p}| \approx 1$ in the higher-order coefficient $\text{Re}b_i$. The effective mass is defined by $m_{\text{eff}}^2 \equiv p_0^2 - |\vec{p}|^2$ from which we can see the correspondence $\tilde{m} \sim m_{\text{eff}}$. While the above simple derivation gives us a clear sense that \tilde{m}_i works as an effective mass at finite temperatures, more precise computation from the poles $\text{Re}\Delta_\pm = 0$ shows that the solutions can be well approximately by two modes: $p_0^2 - |\vec{p}|^2 \approx 0$ and $p_0^2 - |\vec{p}|^2 \approx 2\tilde{m}_i^2$ [116–118], which is valid for soft momentum $p_0 \sim |\vec{p}| \sim gT$. The second mode, which is lepton-flavor dependent, leads to a nonzero CP-violating rate after summing the lepton flavors in Fig. 3.

In the presence of new physics from Eq. (2.2), the lepton thermal masses would get modified. Nevertheless, since neutrino genesis typically culminates at $T < m_\phi$, we expect the thermal correction from Eq. (2.2) would be suppressed by the scalar mass. To see this, let us calculate the contribution from Eq. (2.2) to the real coefficients $\text{Re}a, \text{Re}b$, which is determined by the real part of the one-loop lepton self-energy diagram, as shown in Fig. 9. Following Refs. [112, 118], we arrive at

$$\text{Re}\Sigma_{\ell_i}^T(p) = 2\pi|y_i|^2 \int \frac{d^4q}{(2\pi)^4} \left\{ \frac{\delta[q'^2 - m_\phi^2]}{q^2} f_\phi^{\text{eq}}(|q'_0|) - \frac{\delta(q^2)}{q'^2 - m_\phi^2} f_{\nu_R}^{\text{eq}}(|q_0|) \right\} P_R \not{q} P_L, \quad (\text{B.12})$$

where $|y_i|^2 \equiv \sum_\alpha |y_{i\alpha}|^2$, $q' = q - p$, and we have used the thermal scalar distribution for simplicity. The above integral can be further simplified by taking the transformation $q \rightarrow -q + p$ in the scalar term such that the distribution functions depend only on $|q_0|$.

For soft leptons with $|p_0| \sim |\vec{p}| \sim |y_i|T$, the amplitude given in Eq. (B.12) has a more complicated structure than the usual situation where no vacuum mass appears, as now it introduces a mass scale beyond the HTL treatment. Nevertheless, forbidden neutrino genesis occurs at $T < m_\phi$, which allows us to estimate the modification from Eq. (B.12) to the lepton thermal mass by treating T/m_ϕ as a small parameter. Numerically, this treatment is justified even if the q -momentum integration in Eq. (B.12) is extended to $p \rightarrow \infty$, since the distribution functions $f_{\nu_R}^{\text{eq}}$ and f_ϕ^{eq} ensure that the integral at $q \gg T$ would be exponentially suppressed.

With the general expression for $\text{Re}a, \text{Re}b$ [118]:

$$\text{Re}a_i = \frac{1}{2|\vec{p}|^2} (\text{Tr}[\not{p}\text{Re}\Sigma_{\ell_i}^T] - p_0\text{Tr}[\not{p}\text{Re}\Sigma_{\ell_i}^T]), \quad (\text{B.13})$$

$$\text{Re}b_i = -\frac{1}{2|\vec{p}|^2} (p_0\text{Tr}[\not{p}\text{Re}\Sigma_{\ell_i}^T] - (p_0^2 - |\vec{p}|^2)\text{Tr}[\not{p}\text{Re}\Sigma_{\ell_i}^T]), \quad (\text{B.14})$$

it is straightforward to derive $\text{Re}a_i, \text{Re}b_i$ at leading order of T/m_ϕ . We have

$$\text{Re}a_i = \frac{|y_i|^2}{|\vec{p}|^2} \left[R_{T/m_\phi,1}(|\vec{p}|^2 + 3p_0^2) + R_{T/m_\phi,2}p_0^2 \right], \quad (\text{B.15})$$

$$\text{Re}b_i = -\frac{|y_i|^2}{|\vec{p}|} \left[R_{T/m_\phi,1}(|\vec{p}|^2 + 3p_0^2) \frac{p_0}{|\vec{p}|} + R_{T/m_\phi,2}(p_0^2 - |\vec{p}|^2) \frac{p_0}{|\vec{p}|} \right], \quad (\text{B.16})$$

where $R_{T/m_\phi,1}$ and $R_{T/m_\phi,2}$ denote the T/m_ϕ functions at leading order:

$$R_{T/m_\phi,1} = -\frac{1}{\sqrt{2\pi^3}} \left(\frac{T}{m_\phi} \right)^{5/2} e^{-m_\phi/T} - \frac{7\pi^2}{360} \left(\frac{T}{m_\phi} \right)^4, \quad (\text{B.17})$$

$$R_{T/m_\phi,2} = -\frac{1}{\sqrt{8\pi^3}} \left(\frac{T}{m_\phi} \right)^{3/2} e^{-m_\phi/T} + \frac{7\pi^2}{120} \left(\frac{T}{m_\phi} \right)^4. \quad (\text{B.18})$$

To see how lepton thermal masses are modified, it is instructive to make a comparison between Eqs. (B.15)-(B.16) and Eqs. (B.8)-(B.9). Noticeably, due to the presence of $p_0^2 \sim |\vec{p}|^2 \sim |y_i|^2 T^2$ in Eqs. (B.15)-(B.16), we can infer from Eq. (B.11) that the modified dispersion relation is of higher order in neutrino Yukawa couplings:

$$p_0 - |\vec{p}| \simeq \frac{|y_i|^4 T^2}{|\vec{p}|} \left(R_{T/m_\phi,1} + R_{T/m_\phi,2} \right). \quad (\text{B.19})$$

Given that $|y_i| = \mathcal{O}(0.01)$ is predicted in the case of one nonthermal ν_R , we see that the thermal mass correction from neutrino Yukawa couplings would give

$$\frac{\tilde{m}^2}{T^2} = \mathcal{O}(10^{-8}) \left(R_{T/m_\phi,1} + R_{T/m_\phi,2} \right), \quad (\text{B.20})$$

which is smaller than the contribution from the muon Yukawa coupling $y_\mu^2 = \mathcal{O}(10^{-7})$ at $T < m_\phi$. Therefore, if forbidden neutrinogenesis culminates at $T < m_\phi$, as confirmed by Fig. 6, the maximally resonant enhancement from quasi-degenerate thermal masses, i.e., taking $j = \mu, i = e$ in Eq. (3.34), will not be violated by a large neutrino Yukawa coupling at $\mathcal{O}(0.01)$,

Finally, we would like to comment on the thermal width of soft leptons. The zero-width approximation, $\text{Im}\Delta_\pm \rightarrow 0$, has been used to calculate the CP-violating source, which leads to the on-shell resummed propagators:

$$i\mathcal{S}_i^R(p) \Big|_{\text{onshell}} \approx \pi \text{sign}(p_0) \delta(p^2 - 2\tilde{m}_i^2) \not{p}, \quad (\text{B.21})$$

$$i\mathcal{S}_i^<(p) \Big|_{\text{onshell}} \approx -2\pi \text{sign}(p_0) f(p_0) \delta(p^2 - 2\tilde{m}_i^2) \not{p}, \quad (\text{B.22})$$

$$i\mathcal{S}_i^>(p) \Big|_{\text{onshell}} \approx 2\pi \text{sign}(p_0) [1 - f(p_0)] \delta(p^2 - 2\tilde{m}_i^2) \not{p}, \quad (\text{B.23})$$

where the common pole of \mathcal{S}^R and $\mathcal{S}^<$ is determined by $\text{Re}\Delta_\pm = 0$, with

$$p_0 = \mp \left[|\vec{p}| + \frac{\tilde{m}^2}{|\vec{p}|} - \frac{\tilde{m}^4}{2|\vec{p}|^3} \log \left(\frac{2|\vec{p}|^2}{\tilde{m}^2} \right) + \mathcal{O}(\tilde{m}^6) \right]. \quad (\text{B.24})$$

As elaborated in Ref. [13], including $\text{Im}\Delta_{\pm}$ at next-to-leading order of gauge couplings would give rise to $\text{Im}\Delta_{\pm} = \kappa(3g_2^2 + g_1^2)\tilde{m}^2/|\vec{p}|$ with $\kappa \ll 1$, which protects the stability of the resonant enhancement from finite thermal width near the pole.

C CP-violating rate from three nonthermal neutrinos

This appendix collects the derivation of the CP-violating rate in the case of three nonthermal neutrinos, as given in Eq. (3.29) and Eq. (3.30).

Based on Eq. (3.5), we can write down the CP-violating source \mathcal{S}_{CP} as

$$\mathcal{S}_{\text{CP}}(p) = \frac{1}{2} \int_p (2\pi)\delta(p^2)\text{Tr}[(\mathcal{K}_1 + \mathcal{K}_2)P_R\not{p}P_L], \quad (\text{C.1})$$

where

$$\mathcal{K}_1 \equiv \theta(-p_0)i\mathcal{Y}_{\nu_\alpha}^> - \theta(p_0)i\mathcal{Y}_{\nu_\alpha}^< = -2 \int_{p_\ell} \int_{p_\phi} (2\pi)^4 \delta^4(p - p_\ell + p_\phi) \sum_{i=1}^5 \mathcal{I}_i, \quad (\text{C.2})$$

$$\mathcal{K}_2 \equiv (i\mathcal{Y}_{\nu_\alpha}^> - i\mathcal{Y}_{\nu_\alpha}^<) \mathcal{F}_\alpha = -2\mathcal{F}_\alpha \int_{p_\ell} \int_{p_\phi} (2\pi)^4 \delta^4(p - p_\ell + p_\phi) \sum_{i=1}^5 \mathcal{J}_i, \quad (\text{C.3})$$

with \mathcal{F}_α a neutrino-distribution dependent function: $\mathcal{F}_\alpha \equiv \theta(p_0)f_\alpha(p_0) + \theta(-p_0)\bar{f}_\alpha(-p_0)$. The \mathcal{K}_1 contribution is independent of the neutrino distribution functions f_α . We will mostly follow the approach presented in Ref. [13] to calculate the \mathcal{K}_1 term, and then we extend the approach to determine the \mathcal{K}_2 contribution that depends on f_α, \bar{f}_α .

Let us first consider the \mathcal{K}_1 term. Functions \mathcal{I}_i in \mathcal{K}_1 result from the difference of Eq. (3.19) and Eq. (3.20), and are given by

$$\mathcal{I}_1 = i\mathcal{S}_{\ell_i}^R \left[y_4^* \theta(-p_0) e^{p_{\ell 0}/T} iG_\phi^<(-i\mathcal{Y}_\ell^T) + y_4 \theta(p_0) iG_\phi^>(-i\mathcal{Y}_\ell^T) \right] i\mathcal{S}_{\ell_j}^<, \quad (\text{C.4})$$

$$\mathcal{I}_2 = -i\mathcal{S}_{\ell_i}^R \left[y_4^* \theta(-p_0) iG_\phi^<(-i\mathcal{Y}_\ell^>) - y_4 \theta(p_0) iG_\phi^>(-i\mathcal{Y}_\ell^<)) \right] i\mathcal{S}_{\ell_j}^R, \quad (\text{C.5})$$

$$\mathcal{I}_3 = -i\mathcal{S}_{\ell_i}^R \left[y_4 \theta(-p_0) iG_\phi^<(-i\mathcal{Y}_\ell^>) - y_4^* \theta(p_0) iG_\phi^>(-i\mathcal{Y}_\ell^<)) \right] i\mathcal{S}_{\ell_j}^<, \quad (\text{C.6})$$

$$\mathcal{I}_4 = -i\mathcal{S}_{\ell_i}^R \left[y_4^* \theta(-p_0) e^{p_{\ell 0}/T} iG_\phi^<(-i\mathcal{Y}_\ell^>) - y_4 \theta(p_0) e^{p_{\ell 0}/T} iG_\phi^>(-i\mathcal{Y}_\ell^<)) \right] i\mathcal{S}_{\ell_j}^<, \quad (\text{C.7})$$

$$\mathcal{I}_5 = -i\mathcal{S}_{\ell_i}^R \left[y_4 \theta(-p_0) e^{p_{\ell 0}/T} iG_\phi^<(-i\mathcal{Y}_\ell^{\bar{T}}) + y_4^* \theta(p_0) iG_\phi^>(-i\mathcal{Y}_\ell^{\bar{T}}) \right] i\mathcal{S}_{\ell_j}^<. \quad (\text{C.8})$$

The appearance of $e^{p_{\ell 0}/T}$ in $\mathcal{I}_1, \mathcal{I}_4$ and \mathcal{I}_5 arises from the KMS relation

$$\mathcal{S}_\ell^>(p) = -e^{p_0/T} \mathcal{S}_\ell^<(p), \quad (\text{C.9})$$

which is valid by neglecting small chemical potentials in thermal lepton distribution functions. The detailed calculations of each \mathcal{I}_i can be found in Ref. [13]. The CP-violating source \mathcal{S}_{CP} from the

\mathcal{K}_1 term gives

$$S_{\text{CP}}^{\mathcal{K}_1}(p) = -\frac{(2\pi)^2 \text{Im}(y_4) m_\phi^4}{\tilde{m}_j^2 - \tilde{m}_i^2} \int_{p_i} \tilde{\delta}^4 \left(\sum p_i \right) \delta(p^2) \theta(p_0) \theta(-p_{\ell 0}) \delta(p_\ell^2 - 2\tilde{m}_j^2) iG_\phi^> \mathcal{TC}, \quad (\text{C.10})$$

where $p_i = p, p_\ell, p_\phi$, $\tilde{\delta}^4(\sum p_i) \equiv (2\pi)^4 \delta^4(p - p_\ell + p_\phi)$ dictates energy-momentum conservation, $\sqrt{2\tilde{m}_j}$ corresponds to the effective thermal mass of lepton flavor j [114, 116, 118] with \tilde{m} given by Eq. (B.10), and the *thermal-criterion* function \mathcal{TC} reads

$$\mathcal{TC} \equiv (i\Sigma_\ell^> - i\Sigma_\ell^<) f_\ell^{\text{eq}}(p_{\ell 0}) + i\Sigma_\ell^<. \quad (\text{C.11})$$

This function provides a clear criterion to check whether the CP-violating source is generated in thermal equilibrium. If both ϕ and $\nu_\beta (\nu_\beta \neq \nu_\alpha)$ in the inner loop are in full thermal equilibrium, the KMS relation holds:

$$\Sigma_\ell^>(p_\ell) = -e^{p_{\ell 0}/T} \Sigma_\ell^<(p_\ell), \quad (\text{C.12})$$

and \mathcal{TC} vanishes:

$$\mathcal{TC}^{\text{eq}} = [i\Sigma_\ell^>{}^{\text{eq}}(p_\ell) - i\Sigma_\ell^<{}^{\text{eq}}(p_\ell)] f_\ell^{\text{eq}}(p_{\ell 0}) + i\Sigma_\ell^<{}^{\text{eq}}(p_\ell) = 0. \quad (\text{C.13})$$

It indicates that taking a nonthermal neutrino flavor $\alpha (\neq \beta)$ is not sufficient to induce a nonzero CP-violating source, and there must be additional nonthermal conditions provided by the inner-loop particles.

The quartic scalar mass appearing in Eq. (C.10) comes from the Dirac trace:

$$\text{Tr}[P_L \not{p}_\ell P_R \not{q} P_L \not{p}_\ell P_R \not{p}] = 4(p \cdot p_\ell)(q \cdot p_\ell) - 2p_\ell^2(p \cdot q) \approx m_\phi^4, \quad (\text{C.14})$$

where m_ϕ in the final approximation should be taken by the vacuum mass. To see this, recall that the outer-loop scalar, like the soft leptons, should be also resummed. Due to the spin-0 nature, the scalar thermal mass can be simply added to the vacuum mass,

$$m_\phi^2 = \mu_2^2 + m_{\phi,T}^2, \quad (\text{C.15})$$

$$m_{\phi,T}^2 = \left(\frac{3}{16} g_2^2 + \frac{1}{16} g_1^2 \right) T^2, \quad (\text{C.16})$$

where we only include the corrections from gauge interactions [119]. The thermal scalar mass $m_{\phi,T}$ will cancel the lepton thermal mass $\sqrt{2\tilde{m}}$ in the 4-momentum product $p \cdot p_\ell$ and $q \cdot p_\ell$. On the other hand, forbidden neutrino genesis is an IR-dominated process, which culminates at $T = \mathcal{O}(m_\phi)$. Given this, we neglect the term proportional to $p_\ell^2 = 2\tilde{m}^2$.

To proceed with Eq. (C.10) in the case of three nonthermal ν_R , we define $f_\beta = f_\beta^{\text{eq}} + \delta f_\beta$ ($\delta f_\beta < 0$) for right-handed neutrinos in the inner loop. Then the propagators and self-energy amplitudes can be written as

$$i\mathcal{S}_{\nu_\beta}^{ab}(p) = i\mathcal{S}_{\nu_\beta}^{ab\text{eq}}(p) + i\delta\mathcal{S}_{\nu_\beta}^a(p), \quad (\text{C.17})$$

$$i\mathcal{Y}_\ell^{ab}(p) = i\mathcal{Y}_\ell^{ab\text{eq}}(p) + i\delta\mathcal{Y}_\ell^{ab}(p), \quad (\text{C.18})$$

with $a, b = \pm$, $i\delta\mathcal{S}_{\nu_\beta}^{\pm}(p) = -2\pi\delta(p^2)\not{p}\delta f_\beta(|p_0|)$, and

$$i\mathcal{Y}_\ell^{ab\text{eq}}(p_\ell) = \int_{q, q_\phi} (2\pi)^4 \delta^4(q - q_\phi - p_\ell) P_R i\mathcal{S}_{\nu_\beta}^{ab\text{eq}} P_L iG_\phi^{ba\text{eq}}, \quad (\text{C.19})$$

$$i\delta\mathcal{Y}_\ell^{ab}(p_\ell) = \int_{q, q_\phi} (2\pi)^4 \delta^4(q - q_\phi - p_\ell) P_R i\delta\mathcal{S}_{\nu_\beta}^{\pm} P_L iG_\phi^{ba\text{eq}}, \quad (\text{C.20})$$

with q, q_ϕ the inner-loop momenta of ν_β and ϕ , respectively. Note that we have neglected the quadratic term $\delta\mathcal{S}_{\nu_\beta}^{\pm}\delta G_\phi$, and also the term $\mathcal{S}_{\nu_\beta}^{\text{eq}}\delta G_\phi$. The reason will become clear after we compare the results between the cases of three nonthermal ν_R (section 3.5.1) and one nonthermal ν_R (section 3.5.2). In both cases, $\delta f_\phi = f_\phi - f_\phi^{\text{eq}}$ is expected to be small due to the quasi-thermal nature of the neutrinophilic scalar. Nevertheless, as mentioned in section 3.5.2, a small δf_ϕ can be compensated for by larger Yukawa couplings from the two heavier ν_R . For the case of three nonthermal ν_R , all the neutrino Yukawa couplings are small and hence no coupling enhancement to compensate for the δf_ϕ suppression.

Substituting Eq. (C.18) into Eq. (C.10) and using Eq. (C.13), we can reduce the thermal-criterion function \mathcal{TC} to

$$\mathcal{TC} = -\frac{1}{8\pi p_\ell} \int_{m_\phi^2/(4p_\ell)}^\infty dq \delta f_\beta(q) \left[f_\ell^{\text{eq}}(p_\ell) + f_\phi^{\text{eq}}(q + p_\ell) \right], \quad (\text{C.21})$$

where $q \equiv |\vec{q}|$, $p_\ell \equiv |\vec{p}_\ell|$, and $q_0 > 0, q_{\phi 0} = q_0 - p_{\ell 0} > 0$ were used. The lower integration limit of q comes from the angular integration with $\delta(-m_\phi^2 + 2qp_\ell + 2qp_\ell \cos \theta)$, and we have used $f_\ell(p_{\ell 0}) = 1 - f_\ell(-p_{\ell 0})$, for $p_{\ell 0} = -\omega_j$ with the approximation $\omega_j \approx p_\ell$.

In Eq. (C.10), we can integrate over d^4p via $\delta^4(p - p_\ell + p_\phi)$, $dp_{\ell 0}$ via $\delta(p_\ell^2 - 2\tilde{m}_j^2)$, and $dp_{\phi 0}$ via $\delta(p_\phi^2 - m_\phi^2)$ from the scalar Wightman function $G_\phi^>$. Finally, we arrive at the CP-violating source \mathcal{S}_{CP} from the \mathcal{K}_1 term:

$$\mathcal{S}_{\text{CP}}^{\mathcal{K}_1} = \frac{\text{Im}(y_4)m_\phi^4}{256\pi^4(\tilde{m}_j^2 - \tilde{m}_i^2)} \int_0^\infty \frac{dp_\ell}{p_\ell} \int_{\frac{m_\phi^2}{4p_\ell} + p_\ell}^\infty f_\phi^{\text{eq}}(E_\phi) dE_\phi \int_{\frac{m_\phi^2}{4p_\ell}}^\infty dq \delta f_\beta(q) \left(f_\phi^{\text{eq}} + f_\ell^{\text{eq}} \right), \quad (\text{C.22})$$

where $(f_\phi^{\text{eq}} + f_\ell^{\text{eq}}) \equiv f_\phi^{\text{eq}}(q + p_\ell) + f_\ell^{\text{eq}}(p_\ell)$, and the lower integration limit of E_ϕ comes from the angular integration with $\delta(m_\phi^2 - 2E_\phi p_\ell + 2p_\ell p_\phi \cos \theta)$. Next, let us turn to evaluate the \mathcal{K}_2 term. With the same simplification in calculating \mathcal{I}_i , it is straightforward to obtain the five \mathcal{J}_i functions of \mathcal{K}_2 in Eq. (C.3):

$$\mathcal{J}_1 = i\mathcal{S}_{\ell_i}^R \left[y_4^* e^{p_{\ell 0}/T} iG_\phi^<(-i\mathcal{Y}_\ell^T) + y_4 iG_\phi^>(-i\mathcal{Y}_\ell^T) \right] i\mathcal{S}_{\ell_j}^<, \quad (\text{C.23})$$

$$\mathcal{J}_2 = -i\mathcal{S}_{\ell_i}^R \left[y_4^* iG_\phi^<(-i\mathcal{Y}_\ell^>) - y_4 iG_\phi^>(-i\mathcal{Y}_\ell^<)) \right] i\mathcal{S}_{\ell_j}^R, \quad (\text{C.24})$$

$$\mathcal{J}_3 = -i\mathcal{S}_{\ell_i}^R \left[y_4 iG_\phi^<(-i\mathcal{Y}_\ell^>) - y_4^* iG_\phi^>(-i\mathcal{Y}_\ell^<)) \right] i\mathcal{S}_{\ell_j}^<, \quad (\text{C.25})$$

$$\mathcal{J}_4 = -i\mathcal{S}_{\ell_i}^R \left[y_4^* e^{p_{\ell 0}/T} iG_\phi^<(-i\mathcal{Y}_\ell^>) - y_4 e^{p_{\ell 0}/T} iG_\phi^>(-i\mathcal{Y}_\ell^<)) \right] i\mathcal{S}_{\ell_j}^<, \quad (\text{C.26})$$

$$\mathcal{J}_5 = -i\mathcal{S}_{\ell_i}^R \left[y_4 e^{p_{\ell 0}/T} iG_\phi^<(-i\mathcal{Y}_\ell^T) + y_4^* iG_\phi^>(-i\mathcal{Y}_\ell^T) \right] i\mathcal{S}_{\ell_j}^<. \quad (\text{C.27})$$

To proceed with the \mathcal{K}_2 contribution, we neglect the difference $f_\alpha - \bar{f}_\alpha$, so that $\mathcal{F}_\alpha = f_\alpha(|p_0|)$. This approximation amounts to neglecting the washout rate at two-loop order, which is at $\mathcal{O}(y^4)$ and smaller than $\mathcal{O}(y^2)$ at one-loop order. Writing the CP-violating source from the \mathcal{K}_2 term as

$$\mathcal{S}_{\text{CP}}^{\mathcal{K}_2}(p) = - \int_{p, p_\ell, p_\phi} (2\pi)^5 \delta^4(p - p_\ell + p_\phi) \delta(p^2) \mathcal{F}_\alpha \sum_{i=1}^5 \mathcal{J}_{\text{CP}i}, \quad (\text{C.28})$$

where $\mathcal{J}_{\text{CP}i} \equiv \text{Tr}[\mathcal{J}_i P_R \not{p} P_L]$ with \mathcal{J}_i given by Eqs. (C.23)-(C.27), we arrive at

$$\mathcal{J}_{\text{CP}1} = \frac{2\pi \text{Im}(y_4) m_\phi^4}{\tilde{m}_j^2 - \tilde{m}_i^2} iG_\phi^>(-i\Sigma_\ell^T) \text{sign}(p_{\ell 0}) f_\ell(p_{\ell 0}) \delta(p_\ell^2 - 2\tilde{m}_j^2), \quad (\text{C.29})$$

$$\mathcal{J}_{\text{CP}2} = \frac{i\pi(y_4^* + y_4) m_\phi^4}{\tilde{m}_j^2 - \tilde{m}_i^2} iG_\phi^>(-i\Sigma_\ell^<) \text{sign}(p_{\ell 0}) \delta(p_\ell^2 - 2\tilde{m}_j^2), \quad (\text{C.30})$$

$$\mathcal{J}_{\text{CP}3} = \frac{-\pi[iy_4 + 2\text{Im}(y_4) f_\ell(p_{\ell 0})] m_\phi^4}{\tilde{m}_j^2 - \tilde{m}_i^2} iG_\phi^>(-i\Sigma_\ell^<) \text{sign}(p_{\ell 0}) \delta(p_\ell^2 - 2\tilde{m}_j^2) = \mathcal{J}_{\text{CP}4}, \quad (\text{C.31})$$

$$\mathcal{J}_{\text{CP}5} = \frac{2\pi \text{Im}(y_4) m_\phi^4}{\tilde{m}_j^2 - \tilde{m}_i^2} iG_\phi^>(-i\Sigma_\ell^T) \text{sign}(p_{\ell 0}) f_\ell(p_{\ell 0}) \delta(p_\ell^2 - 2\tilde{m}_j^2). \quad (\text{C.32})$$

Assembling these $\mathcal{J}_{\text{CP}i}$ functions and using the kinetic condition $p_0 p_{\ell 0} < 0$ from Dirac δ -functions, we have

$$\text{sign}(p_{\ell 0}) \mathcal{F}_\alpha = -[\theta(p_0) \theta(-p_{\ell 0}) - \theta(-p_0) \theta(p_{\ell 0})] f_\alpha(|p_0|), \quad (\text{C.33})$$

finally leading us to arrive at

$$\mathcal{S}_{\text{CP}}^{\mathcal{K}_2}(p) = \frac{(2\pi)^3 \text{Im}(y_4) m_\phi^4}{\tilde{m}_j^2 - \tilde{m}_i^2} \int_{p_i} \tilde{\delta}^4 \left(\sum p_i \right) \delta(p^2) \theta(p_0) \theta(-p_{\ell 0}) f_\alpha(|p_0|) \delta_\ell \delta_\phi \mathcal{TC} \quad (\text{C.34})$$

where $p_i = p, p_\ell, p_\phi$, $\tilde{\delta}^4(\sum p_i) \equiv (2\pi)^4 \delta^4(p - p_\ell + p_\phi)$, $\delta_\ell \equiv \delta(p_\ell^2 - 2\tilde{m}_j^2)$, $\delta_\phi \equiv \delta(p_\phi^2 - m_\phi^2)$, and the thermal-criterion function \mathcal{TC} is given by Eq. (C.21). Note that we have performed momentum reflection $p_i \rightarrow -p_i$ in the second term of Eq. (C.33) to obtain Eq. (C.34). Combining Eq. (C.22) and Eq. (C.34) will lead to the final CP-violating rate in the case of three nonthermal ν_R , as given in Eq. (3.29) and Eq. (3.30).

References

- [1] M. Fukugita and T. Yanagida, *Baryogenesis Without Grand Unification*, *Phys. Lett. B* **174** (1986) 45–47.
- [2] M. A. Luty, *Baryogenesis via leptogenesis*, *Phys. Rev. D* **45** (1992) 455–465.
- [3] L. Covi, E. Roulet, and F. Vissani, *CP violating decays in leptogenesis scenarios*, *Phys. Lett. B* **384** (1996) 169–174, [[hep-ph/9605319](#)].
- [4] V. A. Kuzmin, V. A. Rubakov, and M. E. Shaposhnikov, *On the Anomalous Electroweak Baryon Number Nonconservation in the Early Universe*, *Phys. Lett. B* **155** (1985) 36.

- [5] M. D’Onofrio, K. Rummukainen, and A. Tranberg, *Sphaleron Rate in the Minimal Standard Model*, *Phys. Rev. Lett.* **113** (2014), no. 14 141602, [[arXiv:1404.3565](#)].
- [6] G. F. Giudice, A. Notari, M. Raidal, A. Riotto, and A. Strumia, *Towards a complete theory of thermal leptogenesis in the SM and MSSM*, *Nucl. Phys. B* **685** (2004) 89–149, [[hep-ph/0310123](#)].
- [7] W. Buchmuller, P. Di Bari, and M. Plumacher, *Leptogenesis for pedestrians*, *Annals Phys.* **315** (2005) 305–351, [[hep-ph/0401240](#)].
- [8] S. Davidson, E. Nardi, and Y. Nir, *Leptogenesis*, *Phys. Rept.* **466** (2008) 105–177, [[arXiv:0802.2962](#)].
- [9] C. S. Fong, E. Nardi, and A. Riotto, *Leptogenesis in the Universe*, *Adv. High Energy Phys.* **2012** (2012) 158303, [[arXiv:1301.3062](#)].
- [10] E. K. Akhmedov, V. A. Rubakov, and A. Y. Smirnov, *Baryogenesis via neutrino oscillations*, *Phys. Rev. Lett.* **81** (1998) 1359–1362, [[hep-ph/9803255](#)].
- [11] K. Dick, M. Lindner, M. Ratz, and D. Wright, *Leptogenesis with Dirac neutrinos*, *Phys. Rev. Lett.* **84** (2000) 4039–4042, [[hep-ph/9907562](#)].
- [12] C. Cheung and K. M. Zurek, *Affleck-Dine Cogenesis*, *Phys. Rev. D* **84** (2011) 035007, [[arXiv:1105.4612](#)].
- [13] S. Kanemura and S.-P. Li, *Resonant Forbidden CP Asymmetry from Soft Leptons*, [arXiv:2408.06555](#).
- [14] K.-c. Chou, Z.-b. Su, B.-l. Hao, and L. Yu, *Equilibrium and Nonequilibrium Formalisms Made Unified*, *Phys. Rept.* **118** (1985) 1–131.
- [15] E. Calzetta and B. L. Hu, *Nonequilibrium Quantum Fields: Closed Time Path Effective Action, Wigner Function and Boltzmann Equation*, *Phys. Rev. D* **37** (1988) 2878.
- [16] J. Berges, *Introduction to nonequilibrium quantum field theory*, *AIP Conf. Proc.* **739** (2004), no. 1 3–62, [[hep-ph/0409233](#)].
- [17] M. Garny, A. Hohenegger, A. Kartavtsev, and M. Lindner, *Systematic approach to leptogenesis in nonequilibrium QFT: Self-energy contribution to the CP-violating parameter*, *Phys. Rev. D* **81** (2010) 085027, [[arXiv:0911.4122](#)].
- [18] M. Beneke, B. Garbrecht, M. Herranen, and P. Schwaller, *Finite Number Density Corrections to Leptogenesis*, *Nucl. Phys. B* **838** (2010) 1–27, [[arXiv:1002.1326](#)].
- [19] B. Garbrecht, *Leptogenesis: The Other Cuts*, *Nucl. Phys. B* **847** (2011) 350–366, [[arXiv:1011.3122](#)].
- [20] M. Garny, A. Hohenegger, and A. Kartavtsev, *Medium corrections to the CP-violating parameter in leptogenesis*, *Phys. Rev. D* **81** (2010) 085028, [[arXiv:1002.0331](#)].
- [21] M. Beneke, B. Garbrecht, C. Fidler, M. Herranen, and P. Schwaller, *Flavoured Leptogenesis in the CTP Formalism*, *Nucl. Phys. B* **843** (2011) 177–212, [[arXiv:1007.4783](#)].
- [22] M. Drewes and B. Garbrecht, *Leptogenesis from a GeV Seesaw without Mass Degeneracy*, *JHEP* **03** (2013) 096, [[arXiv:1206.5537](#)].
- [23] B. Garbrecht and M. Herranen, *Effective Theory of Resonant Leptogenesis in the Closed-Time-Path Approach*, *Nucl. Phys. B* **861** (2012) 17–52, [[arXiv:1112.5954](#)].
- [24] M. Garny, A. Kartavtsev, and A. Hohenegger, *Leptogenesis from first principles in the resonant regime*, *Annals Phys.* **328** (2013) 26–63, [[arXiv:1112.6428](#)].
- [25] P. S. Bhupal Dev, P. Millington, A. Pilaftsis, and D. Teresi, *Kadanoff–Baym approach to flavour mixing and oscillations in resonant leptogenesis*, *Nucl. Phys. B* **891** (2015) 128–158, [[arXiv:1410.6434](#)].

- [26] T. Frossard, M. Garny, A. Hohenegger, A. Kartavtsev, and D. Mitrouskas, *Systematic approach to thermal leptogenesis*, *Phys. Rev. D* **87** (2013), no. 8 085009, [[arXiv:1211.2140](#)].
- [27] B. Garbrecht, *Leptogenesis from Additional Higgs Doublets*, *Phys. Rev. D* **85** (2012) 123509, [[arXiv:1201.5126](#)].
- [28] T. Hambye and D. Teresi, *Higgs doublet decay as the origin of the baryon asymmetry*, *Phys. Rev. Lett.* **117** (2016), no. 9 091801, [[arXiv:1606.00017](#)].
- [29] E. W. Kolb and S. Wolfram, *Baryon Number Generation in the Early Universe*, *Nucl. Phys. B* **172** (1980) 224. [Erratum: *Nucl.Phys.B* 195, 542 (1982)].
- [30] A. Pilaftsis and T. E. J. Underwood, *Resonant leptogenesis*, *Nucl. Phys. B* **692** (2004) 303–345, [[hep-ph/0309342](#)].
- [31] A. Pilaftsis and T. E. J. Underwood, *Electroweak-scale resonant leptogenesis*, *Phys. Rev. D* **72** (2005) 113001, [[hep-ph/0506107](#)].
- [32] S. Gabriel and S. Nandi, *A New two Higgs doublet model*, *Phys. Lett. B* **655** (2007) 141–147, [[hep-ph/0610253](#)].
- [33] S. M. Davidson and H. E. Logan, *Dirac neutrinos from a second Higgs doublet*, *Phys. Rev. D* **80** (2009) 095008, [[arXiv:0906.3335](#)].
- [34] B. Pontecorvo, *Inverse beta processes and nonconservation of lepton charge*, *Zh. Eksp. Teor. Fiz.* **34** (1957) 247.
- [35] Z. Maki, M. Nakagawa, and S. Sakata, *Remarks on the unified model of elementary particles*, *Prog. Theor. Phys.* **28** (1962) 870–880.
- [36] M. Aoki, S. Kanemura, K. Tsumura, and K. Yagyu, *Models of Yukawa interaction in the two Higgs doublet model, and their collider phenomenology*, *Phys. Rev. D* **80** (2009) 015017, [[arXiv:0902.4665](#)].
- [37] G. C. Branco, P. M. Ferreira, L. Lavoura, M. N. Rebelo, M. Sher, and J. P. Silva, *Theory and phenomenology of two-Higgs-doublet models*, *Phys. Rept.* **516** (2012) 1–102, [[arXiv:1106.0034](#)].
- [38] M. Sher, *Electroweak Higgs Potentials and Vacuum Stability*, *Phys. Rept.* **179** (1989) 273–418.
- [39] S. Nie and M. Sher, *Vacuum stability bounds in the two Higgs doublet model*, *Phys. Lett. B* **449** (1999) 89–92, [[hep-ph/9811234](#)].
- [40] S. Kanemura, T. Kasai, and Y. Okada, *Mass bounds of the lightest CP even Higgs boson in the two Higgs doublet model*, *Phys. Lett. B* **471** (1999) 182–190, [[hep-ph/9903289](#)].
- [41] K. G. Wilson, *Renormalization group and critical phenomena. 2. Phase space cell analysis of critical behavior*, *Phys. Rev. B* **4** (1971) 3184–3205.
- [42] K. Inoue, A. Kakuto, H. Komatsu, and S. Takeshita, *Low-Energy Parameters and Particle Masses in a Supersymmetric Grand Unified Model*, *Prog. Theor. Phys.* **67** (1982) 1889.
- [43] R. F. Dashen and H. Neuberger, *How to Get an Upper Bound on the Higgs Mass*, *Phys. Rev. Lett.* **50** (1983) 1897.
- [44] D. J. E. Callaway, *Nontriviality of Gauge Theories With Elementary Scalars and Upper Bounds on Higgs Masses*, *Nucl. Phys. B* **233** (1984) 189–203.
- [45] M. Luscher and P. Weisz, *Scaling Laws and Triviality Bounds in the Lattice ϕ^4 Theory. 3. N Component Model*, *Nucl. Phys. B* **318** (1989) 705–741.
- [46] S. Kanemura, T. Kubota, and E. Takasugi, *Lee-Quigg-Thacker bounds for Higgs boson masses in a two doublet model*, *Phys. Lett. B* **313** (1993) 155–160, [[hep-ph/9303263](#)].
- [47] A. G. Akeroyd, A. Arhrib, and E.-M. Naimi, *Note on tree level unitarity in the general two Higgs doublet model*, *Phys. Lett. B* **490** (2000) 119–124, [[hep-ph/0006035](#)].

- [48] I. F. Ginzburg and I. P. Ivanov, *Tree-level unitarity constraints in the most general 2HDM*, *Phys. Rev. D* **72** (2005) 115010, [[hep-ph/0508020](#)].
- [49] B. Grinstein, C. W. Murphy, and P. Uttayarat, *One-loop corrections to the perturbative unitarity bounds in the CP-conserving two-Higgs doublet model with a softly broken \mathbb{Z}_2 symmetry*, *JHEP* **06** (2016) 070, [[arXiv:1512.04567](#)].
- [50] D. Toussaint, *Renormalization Effects From Superheavy Higgs Particles*, *Phys. Rev. D* **18** (1978) 1626.
- [51] S. Bertolini, *Quantum Effects in a Two Higgs Doublet Model of the Electroweak Interactions*, *Nucl. Phys. B* **272** (1986) 77–98.
- [52] M. E. Peskin and T. Takeuchi, *A New constraint on a strongly interacting Higgs sector*, *Phys. Rev. Lett.* **65** (1990) 964–967.
- [53] M. E. Peskin and T. Takeuchi, *Estimation of oblique electroweak corrections*, *Phys. Rev. D* **46** (1992) 381–409.
- [54] J. M. Gerard and M. Herquet, *A Twisted custodial symmetry in the two-Higgs-doublet model*, *Phys. Rev. Lett.* **98** (2007) 251802, [[hep-ph/0703051](#)].
- [55] H. E. Haber and D. O’Neil, *Basis-independent methods for the two-Higgs-doublet model III: The CP-conserving limit, custodial symmetry, and the oblique parameters S, T, U*, *Phys. Rev. D* **83** (2011) 055017, [[arXiv:1011.6188](#)].
- [56] S. Kanemura, Y. Okada, H. Taniguchi, and K. Tsumura, *Indirect bounds on heavy scalar masses of the two-Higgs-doublet model in light of recent Higgs boson searches*, *Phys. Lett. B* **704** (2011) 303–307, [[arXiv:1108.3297](#)].
- [57] **ALEPH, DELPHI, L3, OPAL, LEP** Collaboration, G. Abbiendi et al., *Search for Charged Higgs bosons: Combined Results Using LEP Data*, *Eur. Phys. J. C* **73** (2013) 2463, [[arXiv:1301.6065](#)].
- [58] J. A. Harvey and M. S. Turner, *Cosmological baryon and lepton number in the presence of electroweak fermion number violation*, *Phys. Rev. D* **42** (1990) 3344–3349.
- [59] **Planck** Collaboration, N. Aghanim et al., *Planck 2018 results. VI. Cosmological parameters*, *Astron. Astrophys.* **641** (2020) A6, [[arXiv:1807.06209](#)]. [Erratum: *Astron. Astrophys.* 652, C4 (2021)].
- [60] T. Prokopec, M. G. Schmidt, and S. Weinstock, *Transport equations for chiral fermions to order \hbar and electroweak baryogenesis. Part I*, *Annals Phys.* **314** (2004) 208–265, [[hep-ph/0312110](#)].
- [61] T. Prokopec, M. G. Schmidt, and S. Weinstock, *Transport equations for chiral fermions to order \hbar and electroweak baryogenesis. Part II*, *Annals Phys.* **314** (2004) 267–320, [[hep-ph/0406140](#)].
- [62] S.-P. Li, X.-Q. Li, X.-S. Yan, and Y.-D. Yang, *Baryogenesis from hierarchical Dirac neutrinos*, *Phys. Rev. D* **104** (2021), no. 11 115014, [[arXiv:2105.01317](#)].
- [63] **Particle Data Group** Collaboration, S. Navas et al., *Review of particle physics*, *Phys. Rev. D* **110** (2024), no. 3 030001.
- [64] I. Esteban, M. C. Gonzalez-Garcia, M. Maltoni, I. Martinez-Soler, J. a. P. Pinheiro, and T. Schwetz, *NuFit-6.0: Updated global analysis of three-flavor neutrino oscillations*, [arXiv:2410.05380](#).
- [65] W. Buchmuller and S. Fredenhagen, *Quantum mechanics of baryogenesis*, *Phys. Lett. B* **483** (2000) 217–224, [[hep-ph/0004145](#)].
- [66] H. A. Weldon, *Simple Rules for Discontinuities in Finite Temperature Field Theory*, *Phys. Rev. D* **28** (1983) 2007.

- [67] S.-P. Li, X.-Q. Li, X.-S. Yan, and Y.-D. Yang, *Freeze-in Dirac neutrino genesis: thermal leptonic CP asymmetry*, *Eur. Phys. J. C* **80** (2020), no. 12 1122, [[arXiv:2005.02927](#)].
- [68] **T2K** Collaboration, K. Abe et al., *Measurements of neutrino oscillation parameters from the T2K experiment using 3.6×10^{21} protons on target*, *Eur. Phys. J. C* **83** (2023), no. 9 782, [[arXiv:2303.03222](#)].
- [69] **T2K, Super-Kamiokande** Collaboration, K. Abe et al., *First joint oscillation analysis of Super-Kamiokande atmospheric and T2K accelerator neutrino data*, [arXiv:2405.12488](#).
- [70] **NOvA** Collaboration, M. A. Acero et al., *Expanding neutrino oscillation parameter measurements in NOvA using a Bayesian approach*, *Phys. Rev. D* **110** (2024), no. 1 012005, [[arXiv:2311.07835](#)].
- [71] R. L. Kobes and G. W. Semenoff, *Discontinuities of Green Functions in Field Theory at Finite Temperature and Density*, *Nucl. Phys. B* **260** (1985) 714–746.
- [72] R. L. Kobes and G. W. Semenoff, *Discontinuities of Green Functions in Field Theory at Finite Temperature and Density. 2*, *Nucl. Phys. B* **272** (1986) 329–364.
- [73] P. Gondolo and G. Gelmini, *Cosmic abundances of stable particles: Improved analysis*, *Nucl. Phys. B* **360** (1991) 145–179.
- [74] **Simons Observatory** Collaboration, P. Ade et al., *The Simons Observatory: Science goals and forecasts*, *JCAP* **02** (2019) 056, [[arXiv:1808.07445](#)].
- [75] E. Bertuzzo, Y. F. Perez G., O. Sumensari, and R. Zukanovich Funchal, *Limits on Neutrinophilic Two-Higgs-Doublet Models from Flavor Physics*, *JHEP* **01** (2016) 018, [[arXiv:1510.04284](#)].
- [76] **COMET** Collaboration, R. Abramishvili et al., *COMET Phase-I Technical Design Report*, *PTEP* **2020** (2020), no. 3 033C01, [[arXiv:1812.09018](#)].
- [77] **MEG II** Collaboration, A. M. Baldini et al., *The design of the MEG II experiment*, *Eur. Phys. J. C* **78** (2018), no. 5 380, [[arXiv:1801.04688](#)].
- [78] A. Blondel et al., *Research Proposal for an Experiment to Search for the Decay $\mu \rightarrow eee$* , [arXiv:1301.6113](#).
- [79] S.-P. Li, X.-Q. Li, X.-S. Yan, and Y.-D. Yang, *Cosmological imprints of Dirac neutrinos in a keV-vacuum 2HDM**, *Chin. Phys. C* **47** (2023), no. 4 043109, [[arXiv:2202.10250](#)].
- [80] E. Arganda and M. J. Herrero, *Testing supersymmetry with lepton flavor violating tau and mu decays*, *Phys. Rev. D* **73** (2006) 055003, [[hep-ph/0510405](#)].
- [81] A. Ilakovac, A. Pilaftsis, and L. Popov, *Charged lepton flavor violation in supersymmetric low-scale seesaw models*, *Phys. Rev. D* **87** (2013), no. 5 053014, [[arXiv:1212.5939](#)].
- [82] Z.-j. Tao, *Radiative seesaw mechanism at weak scale*, *Phys. Rev. D* **54** (1996) 5693–5697, [[hep-ph/9603309](#)].
- [83] E. Ma, *Verifiable radiative seesaw mechanism of neutrino mass and dark matter*, *Phys. Rev. D* **73** (2006) 077301, [[hep-ph/0601225](#)].
- [84] M. Aoki, S. Kanemura, and O. Seto, *Neutrino mass, Dark Matter and Baryon Asymmetry via TeV-Scale Physics without Fine-Tuning*, *Phys. Rev. Lett.* **102** (2009) 051805, [[arXiv:0807.0361](#)].
- [85] M. Aoki, S. Kanemura, and O. Seto, *A Model of TeV Scale Physics for Neutrino Mass, Dark Matter and Baryon Asymmetry and its Phenomenology*, *Phys. Rev. D* **80** (2009) 033007, [[arXiv:0904.3829](#)].
- [86] M. Aoki, S. Kanemura, and K. Yagyu, *Triviality and vacuum stability bounds in the three-loop neutrino mass model*, *Phys. Rev. D* **83** (2011) 075016, [[arXiv:1102.3412](#)].

- [87] T. Toma and A. Vicente, *Lepton Flavor Violation in the Scotogenic Model*, *JHEP* **01** (2014) 160, [[arXiv:1312.2840](#)].
- [88] K. Enomoto, S. Kanemura, and S. Taniguchi, *The electric dipole moment in a model for neutrino mass, dark matter and baryon asymmetry of the Universe*, [arXiv:2403.13613](#).
- [89] S. Kanemura, Y. Mura, and G. Ying, *Revisiting the model for radiative neutrino masses with dark matter in the $U(1)_{B-L}$ gauge theory*, [arXiv:2410.22835](#).
- [90] **MEG** Collaboration, A. M. Baldini et al., *Search for the lepton flavour violating decay $\mu^+ \rightarrow e^+\gamma$ with the full dataset of the MEG experiment*, *Eur. Phys. J. C* **76** (2016), no. 8 434, [[arXiv:1605.05081](#)].
- [91] **SINDRUM** Collaboration, U. Bellgardt et al., *Search for the Decay $\mu^+ \rightarrow e^+e^+e^-$* , *Nucl. Phys. B* **299** (1988) 1–6.
- [92] S. M. Davidson and H. E. Logan, *LHC phenomenology of a two-Higgs-doublet neutrino mass model*, *Phys. Rev. D* **82** (2010) 115031, [[arXiv:1009.4413](#)].
- [93] A. G. Akeroyd et al., *Prospects for charged Higgs searches at the LHC*, *Eur. Phys. J. C* **77** (2017), no. 5 276, [[arXiv:1607.01320](#)].
- [94] S. Kanemura and C. P. Yuan, *Testing supersymmetry in the associated production of CP odd and charged Higgs bosons*, *Phys. Lett. B* **530** (2002) 188–196, [[hep-ph/0112165](#)].
- [95] Q.-H. Cao, S. Kanemura, and C. P. Yuan, *Associated production of CP odd and charged Higgs bosons at hadron colliders*, *Phys. Rev. D* **69** (2004) 075008, [[hep-ph/0311083](#)].
- [96] *Physics and Detectors at CLIC: CLIC Conceptual Design Report*, [arXiv:1202.5940](#).
- [97] **CLIC** Collaboration, J. de Blas et al., *The CLIC Potential for New Physics*, [arXiv:1812.02093](#).
- [98] **ILC** Collaboration, G. Aarons et al., *International Linear Collider Reference Design Report Volume 2: Physics at the ILC*, [arXiv:0709.1893](#).
- [99] **ILC** Collaboration, *The International Linear Collider Technical Design Report - Volume 2: Physics*, [arXiv:1306.6352](#).
- [100] J. P. Delahaye, M. Diemoz, K. Long, B. Mansoulié, N. Pastrone, L. Rivkin, D. Schulte, A. Skrinsky, and A. Wulzer, *Muon Colliders*, [arXiv:1901.06150](#).
- [101] C. Accettura et al., *Towards a muon collider*, *Eur. Phys. J. C* **83** (2023), no. 9 864, [[arXiv:2303.08533](#)]. [Erratum: *Eur.Phys.J.C* 84, 36 (2024)].
- [102] A. Birkedal, K. Matchev, and M. Perelstein, *Dark matter at colliders: A Model independent approach*, *Phys. Rev. D* **70** (2004) 077701, [[hep-ph/0403004](#)].
- [103] C. Bartels, M. Berggren, and J. List, *Characterising WIMPs at a future e^+e^- Linear Collider*, *Eur. Phys. J. C* **72** (2012) 2213, [[arXiv:1206.6639](#)].
- [104] L. Covi and E. Roulet, *Baryogenesis from mixed particle decays*, *Phys. Lett. B* **399** (1997) 113–118, [[hep-ph/9611425](#)].
- [105] E. Ma and U. Sarkar, *Neutrino masses and leptogenesis with heavy Higgs triplets*, *Phys. Rev. Lett.* **80** (1998) 5716–5719, [[hep-ph/9802445](#)].
- [106] H. Murayama and A. Pierce, *Realistic Dirac leptogenesis*, *Phys. Rev. Lett.* **89** (2002) 271601, [[hep-ph/0206177](#)].
- [107] M. Lindner and M. M. Müller, *Comparison of Boltzmann kinetics with quantum dynamics for a chiral Yukawa model far from equilibrium*, *Phys. Rev. D* **77** (2008) 025027, [[arXiv:0710.2917](#)].
- [108] A. Anisimov, W. Buchmüller, M. Drewes, and S. Mendizabal, *Nonequilibrium Dynamics of Scalar Fields in a Thermal Bath*, *Annals Phys.* **324** (2009) 1234–1260, [[arXiv:0812.1934](#)].

- [109] E. Braaten and R. D. Pisarski, *Soft Amplitudes in Hot Gauge Theories: A General Analysis*, *Nucl. Phys. B* **337** (1990) 569–634.
- [110] J. Frenkel and J. C. Taylor, *High Temperature Limit of Thermal QCD*, *Nucl. Phys. B* **334** (1990) 199–216.
- [111] E. Braaten and R. D. Pisarski, *Simple effective Lagrangian for hard thermal loops*, *Phys. Rev. D* **45** (1992), no. 6 R1827.
- [112] M. E. Carrington, D.-f. Hou, and M. H. Thoma, *Equilibrium and nonequilibrium hard thermal loop resummation in the real time formalism*, *Eur. Phys. J. C* **7** (1999) 347–354, [[hep-ph/9708363](#)].
- [113] M. Bellac, *Thermal Field Theory*. Cambridge University Press, 2000.
- [114] H. A. Weldon, *Effective Fermion Masses of Order gT in High Temperature Gauge Theories with Exact Chiral Invariance*, *Phys. Rev. D* **26** (1982) 2789.
- [115] E. Braaten, R. D. Pisarski, and T.-C. Yuan, *Production of Soft Dileptons in the Quark - Gluon Plasma*, *Phys. Rev. Lett.* **64** (1990) 2242.
- [116] C. P. Kiessig, M. Plumacher, and M. H. Thoma, *Decay of a Yukawa fermion at finite temperature and applications to leptogenesis*, *Phys. Rev. D* **82** (2010) 036007, [[arXiv:1003.3016](#)].
- [117] M. Drewes and J. U. Kang, *The Kinematics of Cosmic Reheating*, *Nucl. Phys. B* **875** (2013) 315–350, [[arXiv:1305.0267](#)]. [Erratum: *Nucl.Phys.B* 888, 284–286 (2014)].
- [118] S.-P. Li, *Dark matter freeze-in via a light fermion mediator: forbidden decay and scattering*, *JCAP* **05** (2023) 008, [[arXiv:2301.02835](#)].
- [119] J. M. Cline, K. Kainulainen, and A. P. Vischer, *Dynamics of two Higgs doublet CP violation and baryogenesis at the electroweak phase transition*, *Phys. Rev. D* **54** (1996) 2451–2472, [[hep-ph/9506284](#)].